# A Solid-State Route to Molecular Clusters: Access to the Solution Chemistry of [Re6Q8]2+ (Q = S, Se) Core-Containing Clusters via Dimensional Reduction

**ARTICLE** *in* JOURNAL OF THE AMERICAN CHEMICAL SOCIETY · MAY 1996

Impact Factor: 12.11 · DOI: 10.1021/ja960216u



**3 AUTHORS**, INCLUDING:

R. H. Holm
Harvard University
**338** PUBLICATIONS **16,549** CITATIONS

# A Solid-State Route to Molecular Clusters: Access to the Solution Chemistry of $[Re_6Q_8]^{2+}$ (Q = S, Se) Core-Containing Clusters via Dimensional Reduction

**Jeffrey R. Long, Logan S. McCarty, and R. H. Holm***

*Contribution from the Department of Chemistry, Harvard University, Cambridge, Massachusetts 02138*

*Received January 22, 1996*[⊗]

**Abstract:** A general method for accessing the solution chemistry of cluster constituents of solid phases exhibiting extended cluster frameworks is demonstrated. The approach is described in terms of simple metal−anion (M−X) frameworks and involves the formal incorporation of AX into a parent structure, resulting in termination of the X bridges between M centers while balancing the charge of the resulting framework with external cations A. The new structures obtained display frameworks of reduced connectedness and dimensionality. By replacing single metal centers with multinuclear cluster cores, this dimensional reduction approach is extended to cluster-containing frameworks. Its utility is demonstrated via application to the phases $Re_6Q_8Cl_2$ (Q = S, Se), exhibiting three- and two-dimensional arrays of face-capped octahedral $[Re_6(\mu_3\text{-}Q)_8]^{2+}$ cluster cores covalently linked through extremely tight $Re_2Q_2$ rhombic interactions of the type common to many intractable cluster frameworks (including the Chevrel phases). Stoichiometric solid-state reactions incorporating TlCl supplement the cores with additional terminal ligands, producing less connected frameworks: two-dimensional $[Re_6Se_8Cl_3]^{1-}$ sheets, one-dimensional $[Re_6Q_8Cl_4]^{2-}$ chains, and ultimately, isolated $[Re_6Q_8Cl_6]^{4-}$ clusters. The connectivities for such $[M_6Q_8]$ frameworks are enumerated; of the 28 possibilities, three previously unknown frameworks are achieved in the structures of $TlRe_6Se_8Cl_3$, $CsRe_6Se_8I_3$, and $Cs_2Re_6Se_8Br_4$, described herein. Alternatively, employing cesium halide as a dimensional reduction agent directly provides the unprecedented molecular clusters in water-soluble form as the phases $Cs_5Re_6S_8X_7$ (X = Cl, Br), $Cs_6Re_6S_8I_8$, and $Cs_4Re_6Se_8I_6$. The species $[Re_6S_8X_6]^{4-}$ (X = Cl, Br, I) are precipitated from aqueous base upon addition of $(Bu_4N)X$ to give the soluble molecular products $(Bu_4N)_4[Re_6S_8Cl_6]$, $(Bu_4N)_4[Re_6S_8Br_6]\cdot H_2O$, and $(Bu_4N)_4[Re_6S_8I_6]\cdot H_2O$. Treatment of yellow acetonitrile solutions of these compounds with anhydrous acid induces an immediate color change to red owing to the formation of the protonated clusters $[Re_6S_7(SH)X_6]^{3-}$. Reversible uptake of a single proton is confirmed by the single-crystal X-ray structure determinations of $(Bu_4N)_3[Re_6S_7(SH)Cl_6]$, $(Bu_4N)_3[Re_6S_7(SH)Br_6]\cdot 2Me_2CO$, and $(Bu_4N)_3[Re_6S_7(SH)I_6]\cdot 2Me_2CO$, as well as spectrophotometric titrations and elemental analyses. The p$K_a$ of $[Re_6S_7(SH)Br_6]^{3-}$ in acetonitrile is estimated at 20. An analogous workup of red $Cs_4Re_6Se_8I_6$ affords $(Bu_4N)_3[Re_6Se_7(SeH)I_6]\cdot 2Me_2CO$.

## Introduction

Large classes of transition metal clusters are produced either exclusively or most reliably by means of high-temperature solid-state reactions.[1,2] Typically, these clusters occur within the confines of an extended covalent framework, requiring that a certain extent of intercluster bond cleavage precede their (potential) liberation from parent solids as discrete molecular units. Over the years, the pursuit of soluble cluster species has resulted in development of an arsenal of low-temperature techniques for excising clusters from such environs.[2] The methods employed generally involve a heterogeneous reaction between the cluster-containing solid and a solution of some appropriate bridge-displacing ligand; however, success is largely contingent upon the accessibility of the clusters within the solid framework. As an instructive example, consider the series of *n*-dimensional phases $Re_6Se_{4+n}Cl_{10-2n}$ ($n = 1-3$). The two-dimensional structure of $Re_6Se_6Cl_6$ (Figure 1) consists of face-capped octahedral $[Re_6Se_6Cl_2]^{4+}$ cores with four Re apices linked to neighboring cores via chloride bridges and the remaining two *trans* Re apices terminated by chloride ligands.[3] When $Re_6Se_6Cl_6$ is stirred in a refluxing acetonitrile solution of $(R_4N)Cl$ (R = Et, Pr), the $Cl^-$ ions displace the bridges between cores, breaking up the extended sheetlike framework to afford a soluble molecular cluster, $[Re_6Se_6Cl_8]^{2-}$.[4] One-dimensional $Re_6Se_5Cl_8$, exhibiting a structure composed of $[Re_6Se_5Cl_3]^{5+}$ cores linked through just two *trans* chloride bridges (the remaining four apices are capped by terminal chloride ligands),[3,5] reacts under similar conditions to yield $[Re_6Se_5Cl_9]^{1-}$.[4] Conversely, the three-dimensional phase $Re_6Se_7Cl_4$, wherein the $[Re_6Se_7Cl]^{3+}$ cores are each linked to six neighbors through chloride bridges,[3,5] has proven inert to a variety of excision techniques; presumably its tightly-packed three-dimensional framework renders the structure impervious to attack by bridge-displacing ligands.[4]

Conspicuously absent in the foregoing discussion is the phase $Re_6Se_8Cl_2$, formulated by extending the series from $Re_6Se_7Cl_4$ with one further substitution of an $Se^{2-}$ for two $Cl^-$ atoms. Its structure (Figure 2) consists of $[Re_6Se_8]^{2+}$ cores, each with two

[⊗] Abstract published in *Advance ACS Abstracts,* May 1, 1996.

(1) (a) Schäfer, H.; Schnering, H. G. *Angew. Chem.* **1964**, *76*, 833. (b) McCarley, R. E. In *Mixed-Valence Compounds*; Brown, D. B., Ed.; D. Reidel: New York, 1980; pp 337−364. (c) Fedorov, V. E.; Mishchenko, A. V.; Fedin, V. P. *Russ. Chem. Rev. (Engl. Transl.)* **1985**, *54*, 408. (d) Simon, A. *Angew. Chem., Int. Ed. Engl.* **1988**, *27*, 159. (e) Perrin, A.; Perrin, C.; Sergent, M. *J. Less-Common Met.* **1988**, *137*, 241. (f) Corbett, J. D. *J. Alloys Compd.* **1995**, *229*, 10.

(2) Lee, S. C.; Holm, R. H. *Angew. Chem., Int. Ed. Engl.* **1990**, *29*, 840 and references therein.

(3) Perrin, A.; Leduc, L.; Sergent, M. *Eur. J. Solid State Inorg. Chem.* **1991**, *28*, 919.

(4) Yaghi, O. M.; Scott, M. J.; Holm, R. H. *Inorg. Chem.* **1992**, *31*, 4778.

(5) Full structural details have not yet been made available.

S0002-7863(96)00216-8 CCC: $12.00 

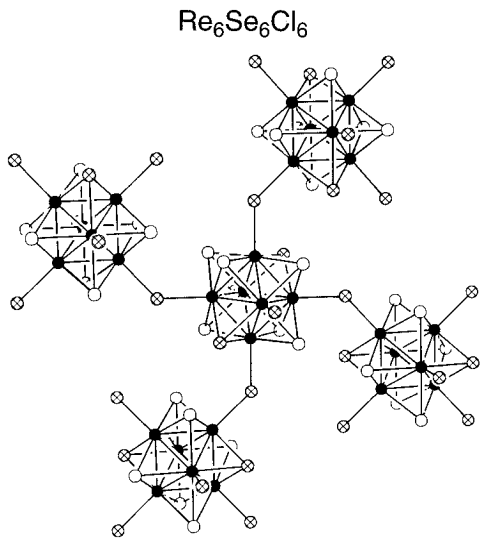


**Figure 1.** Local cluster environment in the $Re_6Se_6Cl_6$ (=$[Re_6Se^i{}_6Cl^i{}_2]Cl^a{}_2Cl^{a\text{-}a}{}_{4/2}$) structure; its sheetlike cluster framework extends within the plane of the page. Black, white, and cross-hatched spheres represent Re, Se, and Cl atoms, respectively. Core Se and Cl atoms are statistically disordered; the positions shown have been arbitrarily designated. Selected mean interatomic distances (Å) and angles (deg) are as follows: Re−Re 2.614(3), Re−$Q^i$ (Q = Se, Cl) 2.506(9), bridging Re−Cl 2.465(7), terminal Re−Cl 2.360, intercore Re−Cl−Re 132.7.[3]

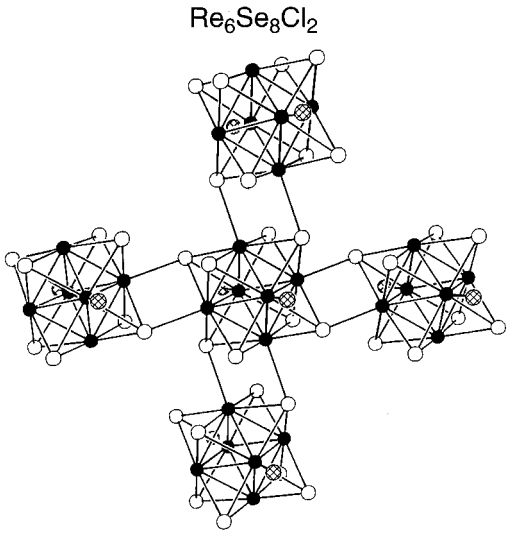


**Figure 2.** Local cluster environment in the structure of $Re_6Se_8Cl_2$ (=$[Re_6Se^i{}_4Se^{i\text{-}a}{}_{4/2}]Se^{a\text{-}i}{}_{4/2}Cl^a{}_2$); the cluster framework extends within the plane of the page. Selected mean interatomic distances (Å) and angles (deg) are as follows: Re−Re 2.64(2), non-rhomb Re−Se 2.52(1), Re−Cl 2.38(1), Re−Re−Re 60.0(5); within $Re_2Se_2$ rhombs Re−Se 2.62-(1), Re···Re 3.43(2).[6]

attendant terminal chlorides at *trans* Re apices, directly linked in two dimensions via rhombic $Re_2Se_2$ interactions.[6] These rigid, compact core−core linkages bestow $Re_6Se_8Cl_2$ with a tightly-bound framework that is completely intractable, despite its two-dimensional nature. As a result of the described differences in framework dimensionality and connectivity, low-temperature excision methods have provided access to the solution chemistry of molecular species containing $[Re_6Se_5Cl_3]^{5+}$ and $[Re_6Se_6Cl_2]^{4+}$ cores,[4] but an analogous chemistry has failed to develop around the $[Re_6Se_7Cl]^{3+}$ and $[Re_6Se_8]^{2+}$ cluster cores.[7] Similarly, the mixed sulfur−chlorine cores $[Re_6S_{4+n}Cl_{4-n}]^{(6-n)+}$ ($n = 1-3$) have been achieved in soluble molecular form,[8] while $[Re_6S_8]^{2+}$ has not. The pure *binary* cores $[Re_6Q_8]^{2+}$ (Q = S, Se) thus present an attractive but unrealized target for study in solution, particularly in view of the complex substitution chemistry associated with the chlorides in the mixed core species.[4,8,9] Such cores are encountered in the phases $Re_6Q_8X_2$ (X = Cl, Br),[6,10] as well as other framework solids, none of which offer a soluble molecular cluster: $Li_4Re_6S_{11}$, $M^I{}_4Re_6Q_{12}$ ($M^I$ = K, Tl), $Cs_4Re_6Q_{13}$, $M^I{}_{10}Re_6S_{14}$ ($M^I$ = Rb, Cs), $Re_6Se_8Te_7$, and $Cs_4Re_6S_{16}$, *inter alia*.[11]

Rhombic intercore linkages of the type observed in $Re_6Se_8Cl_2$ occur in most of the currently intractable cluster frameworks[2] (many containing clusters with no molecular analogues), including the Chevrel phases wherein they link $[Mo_{3n}Q_{3n+2}]^{z-}$ ($n$ = 2−6, 8, 10; Q = S, Se) cores into three-dimensional frameworks.[12] In order to gain access to this realm of cluster chemistry which lies beyond the scope of low-temperature excision techniques or solution synthesis, our recent efforts have focused on the development of a general high-temperature method, termed *dimensional reduction*, for deconstructing solid frameworks.[13] Herein, the concept of dimensional reduction is elaborated and exemplified as an effective means of producing soluble $[Re_6Q_8]^{2+}$ core-containing clusters; initial investigations into the solution properties of these species are also reported.

## Dimensional Reduction

We begin with a development of the concept of dimensional reduction which is more general and detailed than our prior brief introduction to the subject.[13] Thereafter, experimental applications of the concept to certain rhenium−chalcogenide−halide phases are described.

**(a) Metal−Anion Frameworks.** The general premise underlying the approach is exemplified in Figure 3, which illustrates the stepwise deconstruction of a rudimentary three-dimensional metal−anion framework. The initial structure consists of octahedral metal centers, M, covalently linked in three dimensions by bridging anions, X. Successive incorporation of additional equivalents of X reduces the connectivity of

(6) Leduc, P. L.; Perrin, A.; Sergent, M. *Acta Crystallogr*. **1983**, *C39*, 1503.

(7) There are only three reports of cluster excision from three-dimensional solids: (a) Stollmaier, F.; Simon, A. *Inorg. Chem*. **1985**, *24*, 168. (b) Rogel, F.; Corbett, J. D. *J. Am. Chem. Soc*. **1990**, *112*, 8198. (c) Runyan, C. E.; Hughbanks, T. *J. Am. Chem. Soc*. **1994**, *116*, 7909.

(8) (a) Gabriel, J.-C.; Boubekeur, K.; Betail, P. *Inorg. Chem*. **1993**, *32*, 2894. (b) Uriel, S.; Boubekeur, K.; Batail, P.; Orduna, J.; Canadell, E. *Inorg. Chem*. **1995**, *34*, 5307.

(9) Perrin, A. *New J. Chem*. **1990**, *14*, 561.

(10) (a) Speziali, N. L.; Berger, H.; Leicht, G.; Sanjinés, R.; Chapuis, G.; Lévy, F. *Mater. Res. Bull*. **1988**, *23*, 1597. (e) Fischer, C.; Fiechter, S.; Tributsch, H.; Reck, G.; Schultz, B. *Ber. Bunsenges. Phys. Chem*. **1992**, *96*, 1652. (c) Fischer, C.; Alonso-Vante, N.; Fiechter, S.; Tributsch, H. *J. Alloys Compd*. **1992**, *178*, 305.

(11) (a) Bronger, W.; Miessen, H.-J.; Müller, R.; Neugröschel, R. *J. Less-Common Met*. **1985**, *105*, 303. (b) Bronger, W.; Spangenberg, M. *J. Less-Common Met*. **1980**, *76*, 73. (c) Bronger, W.; Miessen, H.-J.; Neugröschel, R.; Schmitz, D.; Spangenberg, M. *Z. Anorg. Allg. Chem*. **1985**, *525*, 41. (d) Huan, G.; Greaney, M.; Tsai, P. P.; Greenblatt, M. *Inorg. Chem*. **1989**, *28*, 2448. (e) Bronger, W.; Loevenich, M.; Schmitz, D.; Schuster, T. *Z. Anorg. Allg. Chem*. **1990**, *587*, 91. (f) Bronger, W.; Kanert, M.; Loevenich, M.; Schmitz, D. *Z. Anorg. Allg. Chem*. **1993**, *619*, 2015. (g) Harbrecht, B.; Selmer, A. *Z. Anorg. Allg. Chem*. **1994**, *620*, 1861. (h) Bronger, W.; Schuster, T. *Z. Anorg. Allg. Chem*. **1990**, *587*, 74.

(12) Selected references: (a) Chevrel, R.; Sergent, M.; Prigent, J. *J. Solid State Chem*. **1971**, *3*, 515. (b) Gougeon, P.; Padiou, J.; Le Marouille, J. Y.; Potel, M.; Sergent, M. *J. Solid State Chem*. **1984**, *54*, 218. (c) Gougeon, P.; Potel, M.; Padiou, J.; Sergent, M. *Mater. Res. Bull*. **1987**, *22*, 453. (d) Chevrel, R.; Gougeon, P.; Potel, M.; Sergent, M. *J. Solid State Chem*. **1985**, *57*, 25. (e) Gougeon, P.; Padiou, J.; Potel, M.; Sergent, M.; Couach, M. *Ann. Chim. (Paris)* **1984**, *9*, 1083. (f) Gougeon, P.; Peña, O.; Potel, M.; Sergent, M.; Brusetti, R. *Ann. Chim. (Paris)* **1984**, *9*, 1079. (g) Gougeon, P.; Potel, M.; Sergent, M. *Acta Crystallogr*. **1989**, *C45*, 182.

(13) Long, J. R.; Williamson, A. S.; Holm, R. H. *Angew. Chem., Int. Ed. Engl*. **1995**, *34*, 226.

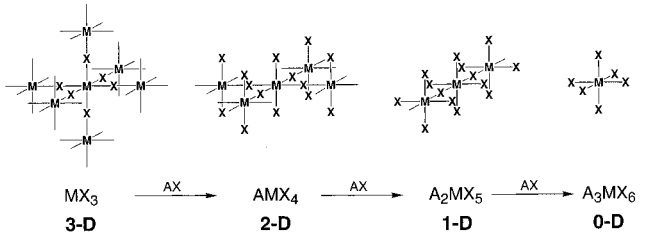


**Figure 3.** Dimensional reduction of $MX_3$ (M = metal, X = bridging anion). By incorporating additional X atoms, the bridges between metals are terminated. Each equivalent added reduces the dimension of the structure by one, and is accompanied by a charge-compensating cation, A. These cations (not shown) reside in the voids between the resulting sheets, chains, and molecules.

the framework by terminating intermetal bridges, producing structures containing sheets, chains, and, finally, discrete molecular units. To preserve the electronic configuration (and subsequently the ligand geometry) of its metal centers, each X added to the structure is accompanied by a charge-compensating cation, A.[14] These cations reside external to the negatively-charged M−X framework (*i.e.*, between anionic sheets, chains, or isolated molecules), and are not depicted in Figure 3. With each equivalent of AX incorporated in the $MX_3$ structure, the overall dimensionality of the ensuing framework is reduced by one—hence the term dimensional reduction. The scheme presented in Figure 3 is not necessarily intended to imply a specific reaction pathway (although it may do so in certain cases), but rather to embody a formalism with which lower-dimensional compounds are readily extrapolated from existing structures.

It is important to emphasize that this formalism does not predict explicit structures. Instead, it utilizes a mode of framework connectivity based upon that of a parent structure, $MX_x$, to predict the connectedness of a new phase, $A_nMX_{x+n}$. The *connectedness* of a framework shall be defined as the mean degree of connectivity of its metal centers (*i.e.*, the mean number of neighboring metals directly connected to a metal center through M−X−M linkages). Consider the $MX_3$ framework at the far left in Figure 3, in which each $MX_6$ octahedron shares all six of its corners with neighboring $MX_6$ octahedra. This structure is efficiently described by the polyhedra connectivity partitioning nomenclature recently introduced.[15,16] The appropriate descriptor is $O_1(1_6)-^3_\infty MX_3$, where the subscript 6 indicates its connectedness. The framework should be viewed as the parent solid whence all possible dimensionally reduced products are derived. Thus, extending our methodology of cluster enumeration,[15] an infinite number of potential substructures[6] may be envisioned, including the three depicted in Figure 3: $O_1(1_4)-^2_\infty[MX_4]^{z-}$, $O_1(1_2)-^1_\infty[MX_5]^{2z-}$, and $O(1_0)-[MX_6]^{3z-}$ (A = $A^{z+}$). Each equivalent of X incorporated reduces the connectedness of the framework by exactly two, permitting formulation of a mean general descriptor

$$O_1(1_{6-2n})-^?_\infty[MX_{3+n}]^{nz-} \qquad 0 < n \le 3 \qquad (1)$$

for any product, $A_nMX_{x+n}$. Such general descriptors will often correspond to a vast number of possible isomeric structures, any one of which might be adopted. For example, the chain $O_1(1_2)-^1_\infty[MX_5]^{2z-}$ in Figure 3 consists of $MX_6$ octahedra sharing *trans* apices. If, instead, the octahedra share *cis* apices, then an isomer with the exact same PCP descriptor emerges, as shown in **1**. From the perspective of the M and X atoms, the

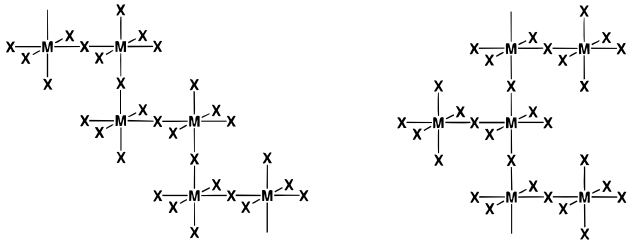

**1** **2**

differences between the two structures are rather subtle and at long range, and the role of the cation A in crystal packing is likely to be a deciding factor in structural preference. So, while dimensional reduction predicts that the connectedness of a phase containing $[MX_5]^{2z-}$ should be two, it does not distinguish between any of the many possible isomeric structures. As mentioned, the connectedness of a framework is actually the *mean* degree of connectivity of its metal centers. For instance, another possible $[MX_5]^{2z-}$ isomer has the $O_1(1_3)-^1_\infty[MX_5]^{2z-}$ chain structure depicted in **2**. This structure contains two nonequivalent octahedral M sites (in equal proportions), one of degree three and the other of degree one, resulting in a mean degree, or connectedness, of two. As indicated in eq 1, the dimensionality of a given phase is structure dependent, and does not necessarily follow from its connectedness (although, obviously, there is an inexact correlation between the two). A zero-dimensional structure, $O_1(4_2)-[M_4X_{20}]^{8z-}$, with empirical formula $[MX_5]^{2z-}$ and a connectedness of two is shown in **3**. Finally, it is worth noting that the value of $n$ in descriptor 1 is not restricted to integers, but may take on any rational number between 0 and 3. In other words, the steps in Figure 3 are not discrete, but represent a numerically (and structurally) convenient sampling from a virtual continuum of empirical formulae. Eradicating a square lattice consisting of one fourth of the total $MX_6$ octahedra from the two-dimensional sheet in Figure 3 results in a new sheet, $O_1(1_42_2)-^2_\infty[M_3X_{14}]^{5z-}$, with the structure shown in **4**. This is just one of the possible structures corresponding to a value of $n = {}^5/_3$ in eq 1; examination of **4** confirms that it does indeed have the predicted connectedness of $6 - 2({}^5/_3) = {}^8/_3$ (for every one $MX_6$ octahedron of degree four, there are two of degree two).

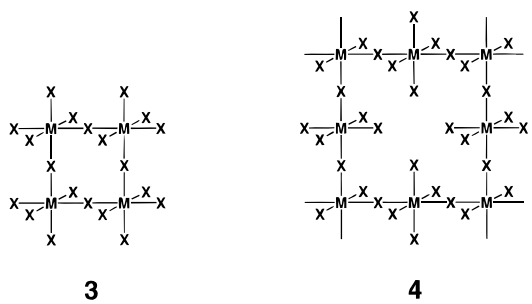

**3** **4**

(14) In general, A will be considerably more electropositive than M.

(15) Long, J. R.; Holm, R. H. *J. Am. Chem. Soc.* **1994**, *116*, 9987.

(16) A brief summation of the PCP notation pertaining only to extended solids follows. Note that the definition for the partitioning has been slightly revised from that previously proposed.[15] Consider a general descriptor with the following formula.

$$P_v(...n_i...)-^d_\infty M_mX_x$$

The descriptor indicates that the structure of the solid $M_mX_x$ contains M centers, with a polyhedral coordination geometry P (P = O for octahedral, T for tetrahedral, and so on, as designated in ref 15), connected to neighboring M centers through linkages consisting of $v$ bridging X atoms. The number $n$ is obtained from the sum of the crystallographic site occupancy factors for any M centers connected in this fashion to exactly $i$ neighboring M centers; all $n$ are scaled by their greatest common denominator to ensure integral values. Finally, $d$ (=1, 2, or 3) specifies the overall dimensionality of the infinitely extended framework.

When applied to a known parent structure, the dimensional reduction formalism may serve both as a means of formulating new synthetic targets of altered connectedness/dimensionality and as a means of relating *established* framework solids throughout chemistry. As an instance of the latter, all four of the structures illustrated in Figure 3 have been demonstrated for the phases $K_nFeF_{3+n}$ ($n = 0, 1, 2, 3$).[17] In addition, the surprisingly diverse crystal chemistry of the ternary ferric fluorides furnishes examples of frameworks **1**−**4**, as encountered in $SrFeF_5$, $BaFeF_5$, $Pb_3Fe_2F_{12}$ (=$Pb_4[Fe_4F_{20}]\cdot 2PbF_2$), and $Na_5Fe_3F_{14}$, respectively.[18] Some further examples are collected in Table 1.[9,19−31] These include a selection of metal oxide, chalcogenide, and halide frameworks featuring a variety of different polyhedra-based connectivity modes. With hundreds of different frameworks based on corner-sharing $SiO_4$ tetrahedra, the silicates represent by far the most thoroughly explored dimensional reduction system.[32] The incorporation of AO in an appropriate $SiO_2$ parent structure invokes a mean general descriptor

$$T_1(1_{4-2n})-^{?}_{\infty}[SiO_{2+n}]^{2n-} \qquad 0 < n \leq 2 \qquad (2)$$

encompassing these many phases.

**(b) Cluster Frameworks.** The basic tenets of dimensional reduction apply equally to frameworks built up from multinuclear cluster cores. Replacing the single metal centers M in Figure 3 with cluster cores of general formula $[M_mQ_q]$ (where Q represents an anionic ligand or atom intimately bonded with multiple intracluster metals, M) leads to the analogous deconstruction of an $[M_mQ_q]X_3$ parent cluster framework. A similar replacement extends the other facets of the formalism (as detailed above for the simpler metal−anion frameworks) to cluster frameworks. Over the years, a number of cluster phases have been structured featuring frameworks readily related by dimensional reduction. These phases, which were not previously correlated by the dimensional reduction argument, are collected in Table 2.[8,33−37] With the exception of $Li_4Re_6S_{11}$, all of the parent phases (those of maximal dimensionality) have proven amenable to cluster excision,[2,7b,8a] rendering the dimensionally reduced products extraneous for purposes of cluster solubilization.

Most of the more intractable cluster frameworks are partially or entirely linked by bonding interactions directly between cores,

**Table 1.** Selected Examples of Solids with Metal−Anion Frameworks Related by Dimensional Reduction

| mode[a] | 3-D | 2-D | 1-D | 0-D | ref |
|---|---|---|---|---|---|
| $S_2$ | PdS | $K_2Pd_3S_4$ | $K_2PdS_2$ | | 19 |
| $T_1$ | $SiO_2$ | $BaSi_2O_5$ | $Na_2SiO_3$ | $K_4SiO_4$ | 20 |
| $T_1$ | | $P_2O_5$ | $NaPO_3$ | $Na_3PO_4$ | 21 |
| $T_1$ | $Ga_2Se_3$ | | | $Cs_8Ga_4Se_{10}$ | 22 |
| $T_1$ | HgS | | $K_2Hg_3S_4$ | $K_6HgS_4$ | 23 |
| $T_2$ | MnS | $K_2Mn_3S_4$ | $K_2MnS_2$ | $K_6MnS_4$ | 24 |
| $T_2$ | $Cu_2Q$[b] | KCuQ[b] | | | 25 |
| $T_2$ | ZnS | $Na_2Zn_3S_4$ | $Na_2ZnS_2$ | $Na_6ZnS_4$ | 26 |
| $SPy_{2,1}$ | | $V_2O_5$ | $KVO_3$ | | 27 |
| $O_1$ | $WO_3$ | | $Ba_2WO_5$ | $Ba_3WO_6$ | 28 |
| $O_1$ | $FeF_3$ | $KFeF_4$ | $K_2FeF_5$ | $K_3FeF_6$ | 17 |
| $O_{2,1}$ | $PtO_2$ | | | $Li_8PtO_6$ | 29 |
| $O_2$ | | $CdCl_2$ | | $K_4CdCl_6$ | 30 |

[a] Principal framework connectivity mode in PCP notation. [b] Q = S, Se.

**Table 2.** Structurally Proven Examples of Solids with Cluster Frameworks Related by Dimensional Reduction

| mode[a] | 3-D | 2-D | 1-D | 0-D | ref |
|---|---|---|---|---|---|
| $Cl^{a-a}$ | | $Re_3Cl_9$ | | $A_3Re_3Cl_{12}$[b] | 33 |
| $Cl^{a-a}$ | $K_2Zr_6BCl_{15}$ | $Cs_3Zr_6BCl_{16}$ | $Ba_2Zr_6BCl_{17}$ | $Rb_5Zr_6BCl_{18}$ | 34 |
| $Cl^{a-a}$ | | $Nb_6Cl_{14}$ | | $K_4Nb_6Cl_{18}$ | 35 |
| $Cl^{a-a}$ | | $Mo_6Cl_{12}$ | $NaMo_6Cl_{13}$ | $PbMo_6Cl_{14}$ | 36 |
| $Cl^{a-a}$ | | | $Re_6S_5Cl_8$ | $RbRe_6S_5Cl_9$ | 8 |
| $S^{a-a}$ | $Li_4Re_6S_{11}$ | | | $A_{10}Re_6S_{14}$[b] | 37 |

[a] Principal cluster framework connectivity mode. [b] A = Rb, Cs.


(17) (a) Hepworth, M. A.; Jack, K. H.; Peacock, R. D.; Westland, G. J. *Acta Crystallogr*. **1957**, 63. (b) Heger, G.; Geller, R.; Babel, D. *Solid State Commun*. **1971**, *9*, 335. (c) Vlasse, M.; Matejka, G.; Tressaud, A.; Wanklyn, B. M. *Acta Crystallogr*. **1977**, *B33*, 3377. (d) Bode, V. H.; Voss, E. *Z. Anorg. Allg. Chem*. **1957**, *290*, 1.

(18) (a) von der Muehll, R.; Daut, F.; Ravez, J. *J. Solid State Chem*. **1973**, *8*, 206. (b) von der Muehll, R.; Andersson, S.; Galy, J. *Acta Crystallogr*. **1971**, *B27*, 2345. (c) Decap, G.; Retoux, R.; Calage, Y. *Z. Anorg. Allg. Chem*. **1993**, *619*, 1850. (d) Vlasse, M.; Menil, F.; Moriliere, C.; Dance, J. M.; Tressaud, A.; Portier, J. *J. Solid. State Chem*. **1976**, *17*, 291.

(19) (a) Brese, N. E.; Squattrito, P. J.; Ibers, J. A. *Acta Crystallogr*. **1985**, *C41*, 1829. (b) Huster, J.; Bronger, W. *J. Solid State Chem*. **1974**, *11*, 254. (c) Bronger, W.; Jäger, S.; Rennau, R.; Schmitz, D. *J. Less-Common Met*. **1989**, *154*, 261.

(20) (a) Wyckoff, R. W. G. *Z. Kristallogr*. **1927**, *63*, 507. (b) Hesse, K.-F.; Liebau, F. *Z. Kristallogr*. **1980**, *153*, 3. (c) McDonald, W. S.; Cruickshank, D. W. *J. Acta Crystallogr*. **1967**, *22*, 37. (d) Bernet, K.; Hoppe, R. *Z. Anorg. Allg. Chem*. **1990**, *589*, 129.

(21) (a) MacGillavry, C. H.; de Decker, H. C. J.; Nijland, L. M. *Nature* **1949**, *164*, 448. (b) McAdam, A.; Jost, K. H.; Beagley, B. *Acta Crystallogr*. **1968**, *B24*, 1621. (c) Wiench, D. M.; Jansen, M. *Z. Anorg. Allg. Chem*. **1980**, *461*, 101.

(22) (a) Lübbers, D.; Leute, V. *J. Solid State Chem*. **1982**, *43*, 399. (b) Deiseroth, H. J. *Z. Kristallogr*. **1984**, *166*, 283.

(23) (a) Huang, T.; Ruoff, A. L. *J. Appl. Phys*. **1983**, *54*, 5459. (b) Kanatzidis, M. G.; Park, Y. *Chem. Mater*. **1990**, *2*, 99. (c) Sommer, H.; Hoppe, R. *Z. Anorg. Allg. Chem*. **1978**, *443*, 201.

(24) (a) Furuseth, S.; Kjekshus, A. *Acta Chem. Scand*. **1965**, *19*, 1405. (b) Bronger, W. *Angew. Chem*. **1966**, *78*, 113. (c) Bronger, W.; Balk-Hardtdegen, H.; Schmitz, D. *Z. Anorg. Allg. Chem*. **1989**, *574*, 99. (d) Bronger, W.; Balk-Hardtdegen, H. *Z. Anorg. Chem*. **1989**, *574*, 99. (d) Bronger, W.; Balk-Hardtdegen, H. *Z. Anorg. Allg. Chem*. **1989**, *574*, 89.

(25) (a) Oliveria, M.; McMullan, R. K.; Wuensch, B. J. *Solid State Ionics* **1988**, *28*, 1332. (b) Savelsberg, G.; Schäfer, H. *Z. Naturforsch*. **1978**, *33B*, 370, 711.

(26) (a) Kisi, E. H.; Elcombe, M. M. *Acta Crystallogr*. **1989**, *C45*, 1867. (b) Bronger, W.; Hendriks, U.; Müller, P. *Z. Anorg. Allg. Chem*. **1988**, *559*, 95. (c) Klepp, K. O.; Bronger, W. *Z. Kristallogr*. **1983**, *162*, 134.

(27) (a) Bachmann, H. G.; Ahmed, F. R.; Barnes, W. H. *Z. Kristallogr*. **1961**, *115*, 110. (b) Hawthorne, F. C.; Calvo, C. J. *J. Solid State Chem*. **1977**, 157.

(28) (a) Salje, E. *Acta Crystallogr*. **1977**, *B33*, 574. (b) Kovba, L. M.; Lykova, L. N.; Balashov, V. L.; Kharlanov, A. L. *Koord. Khim*. **1985**, *11*, 1426. (c) Balashov, V. L.; Kharlanov, A. A.; Kondratov, O. I.; Fomichev, V. V. *Zh. Neorg. Khim*. **1991**, *36*, 456.

(29) (a) Siegel, S.; Hoekstra, H. R.; Tani, B. S. *J. Inorg. Nucl. Chem*. **1969**, *31*, 3803. (b) Kröschell, P.; Wolf, R.; Hoppe, R. *Z. Anorg. Allg. Chem*. **1986**, *536*, 81.

(30) (a) Pauling, L.; Hoard, J. L. *Z. Kristallogr*. **1930**, *74*, 546. (b) Bergerhoff, G.; Schmitz-DuMont, O. *Naturwissenschaften* **1954**, *41*, 280.

(31) The correlation between cation/anion incorporation and dimensionality has been specifically recognized in the structures of certain metal chalcogenides: (a) Kanatzidis, M. G.; Park, Y. *Chem. Mater*. **1990**, *2*, 99. (b) Axtell, E. A.; Liao, J.-H.; Pikramenou, Z.; Park, Y.; Kanatzidis, M. G. *J. Am. Chem. Soc*. **1993**, *115*, 12191. (c) Lu, Y.-J.; Ibers, J. A. *Comments Inorg. Chem*. **1993**, *14*. 229.

(32) Liebau, F. *Structural Chemistry of Silicates*; Springer-Verlag: Berlin, 1985.

(33) (a) Cotton, F. A.; Mague, J. T. *Inorg. Chem*. **1964**, *3*, 1402. (b) Meyer, G.; Irmler, M. *J. Less-Common Met*. **1986**, *119*, 31.

(34) (a) Ziebarth, R. P.; Corbett, J. D. *J. Am. Chem. Soc*. **1988**, *110*, 1132. (b) Ziebarth, R. P.; Corbett, J. D. *Inorg. Chem*. **1989**, *28*, 626. (c) Zhang, J.; Corbett, J. D. *J. Less-Common Met*. **1989**, *156*, 49. (d) Ziebarth, R. P.; Corbett, J. D. *J. Am. Chem. Soc*. **1989**, *111*, 3272.

(35) (a) Simon, A.; Schnering, H. G.; Wöhrle, H.; Schäfer, H. *Z. Anorg. Allg. Chem*. **1965**, *339*, 155. (b) Simon, A.; von Schnering, H.-G.; Schäfer, H. *Z. Anorg. Allg. Chem*. **1968**, *361*, 235.

(36) (a) Schäfer, H.; Schnering, H.-G.; Tillack, J.; Kuhnen, F.; Wöhrle, F.; Baumann, H. *Z. Anorg. Allg. Chem*. **1967**, *353*, 281. (b) Böschen, S.; Keller, H. L. *Z. Kristallogr*. **1991**, *196*, 159. (c) Böschen, S.; Keller, H. L. *Z. Kristallogr*. **1992**, *200*, 305.

(37) (a) Bronger, W.; Miessen, H.-J.; Müller, R.; Neugröschel, R. *J. Less-Common Met*. **1985**, *105*, 303. (b) Bronger, W.; Kanert, M.; Loevenich, M.; Schmitz, D. *Z. Anorg. Allg. Chem*. **1993**, *619*, 2015.

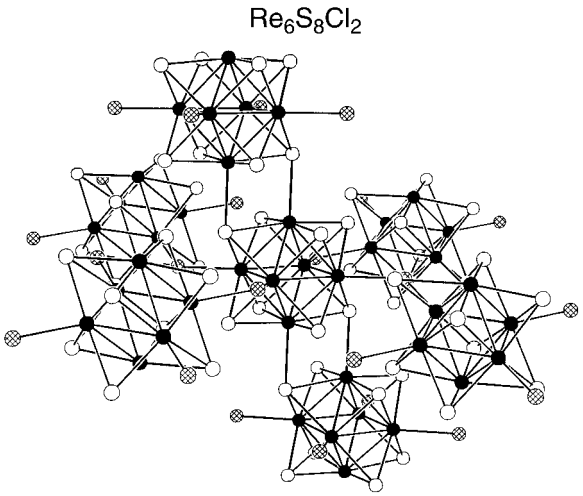


**Figure 4.** Local cluster environment in the three-dimensional $Re_6S_8Cl_2$ (=$[Re_6S^i{}_6S^{i\text{-}a}{}_{2/2}]S^{a\text{-}i}{}_{2/2}Cl^{a\text{-}a}{}_{4/2}$) parent structure. Black, white, and cross-hatched spheres represent Re, S, and Cl atoms, respectively. Selected mean interatomic distances (Å) and angles (deg) are as follows: Re−Re 2.59(1), non-rhomb Re−S 2.39(1), Re−Cl 2.46(1), Re−Re−Re 60.0(4); within $Re_2S_2$ rhombs Re−S 2.50(2).[10b]

rather than through some intermediate bridging atom, as in $Re_6Se_6Cl_6$ (Figure 1) and all of the phases listed in Table 2.[2] The three-dimensional framework of $Re_6S_8Cl_2$ provides such an example. Its structure[10b] is built up from electron-precise face-capped octahedral $[Re_6S_8]^{2+}$ cluster cores, each linked to six neighboring cores via two rhombic $Re_2S_2$ interactions (situated at *trans* apices of the $Re_6$ octahedron) and four $\mu_2$-Cl atoms. Thus, a total of eight bonds astrict each cluster, making the compound impervious to excision. By focusing on the local environment of a single cluster, Figure 4 attempts to convey the connectivity of the framework; however, due to its tightly-packed three-dimensional nature, the drawing is crowded and difficult to penetrate.

A notation specific to cluster frameworks has been developed as an aid in both visualizing structures and unambiguously communicating connectivities.[38] It is now advantageous to provide a brief explanation of this notation, which will be generously employed hereafter. To begin, attention should be directed at a *single* cluster within the framework.[39] Utilizing the $Re_6S_8Cl_2$ structure as an example, consider the central cluster in Figure 4. Square brackets are used to designate the cluster core, which consists of six Re atoms and eight *inner* S ligands. Outer (*ausser*) ligands that are not a part of the core, but which are directly bonded to core metal atoms, are listed outside the brackets.

$$[Re_6S_8]S_2Cl_4 \tag{3}$$

Inner ligands that serve as an outer ligand for a neighboring core are labeled with a superscript "i-a", while those which do not are labeled "i". Outer ligands that serve as an inner or outer ligand for a neighboring core are labeled with a superscript "a-i" or "a-a", respectively, while those which do neither are labeled "a".

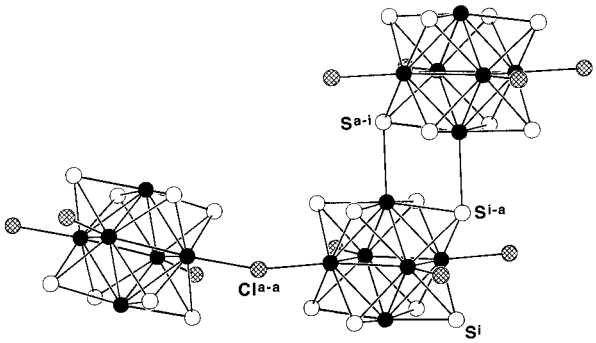


**Figure 5.** A piece of the $Re_6S_8Cl_2$ structure clearly displaying the two different types of intercluster linkages. The various ligand designations present in its cluster connectivity notation are as indicated.

$$[Re_6S^i{}_6S^{i\text{-}a}{}_2]S^{a\text{-}i}{}_2Cl^{a\text{-}a}{}_4 \tag{4}$$

Examples of some of these types of ligands are indicated on a smaller piece of the $Re_6S_8Cl_2$ structure in Figure 5 (the core on the lower right is considered the central cluster). Finally, denominators corresponding to the number of distinct cores to which each type of ligand is bonded are added to the formula (denominators of 1 are omitted).

$$[Re_6S^i{}_6S^{i\text{-}a}{}_{2/2}]S^{a\text{-}i}{}_{2/2}Cl^{a\text{-}a}{}_{4/2} \tag{5}$$

Note that summing the atoms in a correct formulation will always result in the proper stoichiometry.

Like their metal−anion brethren, cluster frameworks can exhibit structural isomerism. The $Re_6S_8Cl_2$ structure is also assumed by the isotypic phases $Re_6S_8Br_2$ and $Re_6Se_8Br_2$;[10] however, for reasons which are not entirely clear, $Re_6Se_8Cl_2$ adopts a different structure. The latter structure[6] (Figure 2) is built up from analogous $[Re_6Se_8]^{2+}$ cores, each with two attendant terminal chlorides ($Cl^a$) at *trans* rhenium apices and four rhombic $Re_2Se_2$ interactions directly linking neighboring cores. The ensuing connectivity notation for this rigid two-dimensional framework is $[Re_6Se^i{}_4Se^{i\text{-}a}{}_{4/2}]Se^{a\text{-}i}{}_{4/2}Cl^a{}_2$. Significantly, the connectedness of both isomeric frameworks is eight.[40]

In general, the excision techniques currently available are only effective for cluster cores linked exclusively through $\mu_2$-halide bridges in frameworks with a connectedness of six or less.[2] Thus, neither $Re_6S_8Cl_2$ nor $Re_6Se_8Cl_2$ is amenable to cluster excision. In view of this, the multitude of solids containing $[Re_6Q_8]^{2+}$ (Q = S, Se) cluster cores,[2] and the lack of any corresponding species in solution, the $Re_6S_8Cl_2$ and $Re_6Se_8Cl_2$ structures were chosen as prototypes for testing the validity of the dimensional reduction approach.

## Experimental Section

**Preparation of Compounds.** The preparation of $Cs_5Re_6S_8Cl_7$ has been reported elsewhere.[13] The reactants Re (−325 mesh, Cerac), S (−100 mesh, Aldrich), Se (−325 mesh, Strem), $ReBr_5$ (−100 mesh, Cerac), $Br_2$ (Fluka), $I_2$ (Strem), HBr (48%, Mallinckrodt), HI (47%, Fluka), $(Bu_4N)X$ (X = Cl, Br, I; Aldrich), $SOCl_2$ (Mallinckrodt), and $SOBr_2$ (Fluka) were used as purchased, without further purification. Alkali metal halides CsBr (Strem) and CsI (−20 mesh, Cerac) were ground and dried for two days at 200 °C prior to use. Fused silica ampules with dimensions i.d. × o.d. × 1 = 7 × 10 × 120 mm were

(38) Schäfer, H.; von Schnering, H. G. *Angew. Chem.* **1964**, *76*, 833.

(39) The notation makes the simplifying assumption that all clusters in the framework are equivalent. This assumption, which will be tentatively adopted here, obliterates many of the intricacies of dimensional reduction considered above for metal−anion frameworks. However, it should be kept in mind that frameworks composed of more than one type of cluster are not entirely unknown; several examples have been uncovered among the Chevrel phases: (a) Chevrel, R.; Sergent, M.; Seeber, B.; Fischer, Ø.; Grüttner, A.; Yvon, K. *Mater. Res. Bull.* **1979**, *14*, 567. (b) Chevrel, R.; Potel, M.; Sergent, M.; Decroux, M.; Fischer, Ø. *J. Solid State Chem.* **1980**, *34*, 247.

(40) Due to the capacity of multinuclear cluster cores for forging multiple bond linkages (see Figure 2), we will now employ a slightly revised definition of connectedness as the minimum number of bonds that must be broken to completely liberate a cluster core from its surrounding framework.

dried overnight at 150 °C. High temperature reactions were carried out in tube furnaces (Marshall, Lindberg or Carbolite) equipped with programmable Eurotherm temperature controllers; furnace temperatures were typically ramped up at 2 °C/min. Products were identified by single crystal X-ray structure determinations and subsequent X-ray powder diffraction (XRPD) patterns. Solid phases exhibiting large crystal faces were subjected to an electron microprobe analysis (EMPA).

**$Cs_5Re_6S_8Br_7$.** Liquid $Br_2$ (*ca*. 0.2 g) was added to a tared fused silica ampule; the ampule and its contents were accurately weighed and cooled with liquid nitrogen. A mixture of Re, S, and CsBr (stoichiometric amounts bringing the total mass of reactants to *ca*. 4 g) was intimately ground and added to the ampule, which was then evacuated and sealed. The sample was heated (with reactants situated at the cooler end of the ampule) at 850 °C for 6000 min, cooled at 0.2 °C/min to about 500 °C, and air-quenched. The product crystallized as thick yellow-orange hexagonal plates. EMPA: $Cs_{5.15(6)}Re_{6.00(5)}S_{8.02(2)}Br_{7.5(2)}$.

**$Cs_6Re_6S_8I_8$.** A fused silica ampule was charged with a *ca*. 2-g mixture of Re, S, $I_2$, and CsI in proportions corresponding to an overall stoichiometry of $Cs_8Re_6S_8I_{10}$ (two extra equivalents of CsI) and sealed under static vacuum. The sample was heated (with reactants situated at the cooler end of the ampule) at 850 °C for 6000 min, cooled at 0.2 °C/min to about 500 °C, and air-quenched. The product crystallized as thick yellow rectangular plates along with CsI and varying amounts of an insoluble black phase of unknown composition. EMPA: $Cs_{6.17(5)}Re_{6.00(9)}S_{7.7(1)}I_{8.25(5)}$.

**$Cs_2Re_6Se_8Br_4$.** A 0.500-g mixture of Re, Se, $ReBr_5$, and CsBr in proportions corresponding to an overall stoichiometry of $Cs_5Re_6Se_8Br_7$ (three extra equivalents of CsBr) was intimately ground in a pure dinitrogen atmosphere and sealed in a fused silica ampule under vacuum. The sample was heated (with reactants situated at the cooler end of the ampule) at 800 °C for 6000 min, cooled at 0.2 °C/min to about 400 °C, and air-quenched. The product crystallized (along with the excess CsBr) as metallic black needles.

**$CsRe_6Se_8I_3$.** A fused silica ampule was charged with a stoichiometric 0.800-g mixture of Re, Se, $I_2$, and CsI and sealed under vacuum. The sample was heated (with reactants situated at the cooler end of the ampule) at 850 °C for 6000 min, cooled at 0.2 °C/min to about 400 °C, and air-quenched. The product crystallized as metallic black elongated rhombic plates. EMPA: $Cs_{1.1(1)}Re_{6.0(1)}Se_{8.0(1)}I_{3.13(8)}$.

**$Cs_4Re_6Se_8I_6$.** A fused silica ampule was charged with a stoichiometric *ca*. 2-g mixture of Re, Se, $I_2$, and CsI and sealed under static vacuum. The sample was heated (with reactants situated at the cooler end of the ampule) at 850 °C for 6000 min, cooled at 0.2 °C/min to about 500 °C, and air-quenched. The product crystallized as thick red rhombic plates. Occasional minor impurities of $CsRe_6Se_8I_3$ (insoluble) and CsI were also observed. EMPA: $Cs_{4.5(2)}Re_{6.0(2)}Se_{7.6(9)}I_{6.4(2)}$.

**$(Bu_4N)_4[Re_6S_8Cl_6]$.** A 1.70-g portion of the product recovered from a reaction targeting $Cs_5Re_6S_8Cl_7$ was pulverized and stirred in 200 mL of 1 M aqueous HCl for 45 min. The mixture was filtered to give a small amount of gray-black solid and a bright yellow filtrate. Solid KOH (26 g, 0.46 mol) was added to the filtrate and stirred until it completely dissolved. Excess $(Bu_4N)Cl$ (*ca*. 1 g) was added to the stirred solution which turned colorless upon formation of a yellow precipitate. The precipitate was collected by filtration and dissolved in 100 mL of acetonitrile to give a yellow-orange solution. The solution was reduced to dryness leaving a yellow-orange solid which was recrystallized by evaporation from a *ca*. 1:1 (v/v) mixture of acetone and toluene. The resulting yellow-orange plates were washed with successive 30-mL aliquots of toluene, water, toluene, and pentane to afford 0.73 g (38%) of product. Absorption spectrum (MeCN): $\lambda_{max}$ ($\epsilon_M$) 377 (sh, 1860), 434 (1050), 537 (140) nm. Anal. Calcd for $C_{64}H_{144}Cl_6N_4S_8Re_6$: C, 30.07; H, 5.68; Cl, 8.32; N, 2.19; Re, 43.70; S, 10.03. Found: C, 29.88; H, 5.59; Cl, 8.38; N, 2.17; Re, 43.88; S, 10.11.

**$(Bu_4N)_3[Re_6S_7(SH)Cl_6]$.** The product recovered (1.96 g) from a reaction targeting $Cs_5Re_6S_8Cl_7$ was pulverized and stirred in 200 mL of 1 M aqueous HCl for 30 min. The mixture was filtered to give a small amount of gray-black solid and a bright yellow filtrate. Excess $(Bu_4N)Cl$ (*ca*. 800 mg) was added to the stirred filtrate which turned colorless upon formation of a yellow precipitate. The precipitate was collected by filtration and dissolved in 100 mL of acetonitrile to give a yellow-orange solution. Several drops of water and *ca*. 0.5 mL of $SOCl_2$ were added to the stirred solution which underwent an immediate color change to red. The solution was reduced to dryness leaving a red solid which was recrystallized by evaporation from a *ca*. 1:1 (v/v) mixture of acetone and toluene. The resulting red plates were washed with successive 30-mL aliquots of toluene, water, toluene, and pentane to afford 1.31 g (66%) of product. Absorption spectrum (MeCN): $\lambda_{max}$ ($\epsilon_M$) 378 (sh, 1820), 489 (785), 544 (1190) nm. Anal. Calcd for $C_{48}H_{109}Cl_6N_3S_8Re_6$: C, 24.91; H, 4.75; Cl, 9.19; N, 1.82; Re, 48.26; S, 11.08. Found: C, 24.83; H, 4.68; Cl, 9.24; N, 1.77; Re, 48.34; S, 11.21.

**$(Bu_4N)_4[Re_6S_8Br_6]\cdot H_2O$.** A 1.17-g portion of the product recovered from a reaction targeting $Cs_5Re_6S_8Br_7$ (as described above) was pulverized and stirred in 200 mL of 1 M aqueous HBr for 30 min. The mixture was filtered to give a small amount of gray-black solid and a bright yellow filtrate. Solid NaOH (26 g, 0.65 mol) was added to the filtrate and the mixture was stirred until the solid completely dissolved. Excess $(Bu_4N)Br$ (*ca*. 600 mg) was added to the stirred solution which turned colorless upon formation of a yellow precipitate. The precipitate was collected by filtration and dissolved in 100 mL of MeCN to give a yellow-orange solution. The solution was reduced to dryness leaving a yellow-orange residue which was crystallized by evaporation from a *ca*. 1:1 (v/v) mixture of acetone and toluene. The resulting yellow-orange plates were washed with successive 30-mL aliquots of toluene, water, toluene, and pentane to afford 0.73 g (58%) of pure product. Absorption spectrum (MeCN): $\lambda_{max}$ ($\epsilon_M$) 401 (sh, 1540), 443 (945), 545 (90) nm. Anal. Calcd for $C_{64}H_{146}Br_6N_4OS_8Re_6$: C, 27.06; H, 5.18; Br, 16.87; N, 1.97; Re, 39.32; S, 9.03. Found: C, 27.15; H, 5.16; Br, 16.76; N, 1.89; Re, 39.26; S, 9.18.

**$(Bu_4N)_3[Re_6S_7(SH)Br_6]$.** The product recovered (3.48 g) from a reaction targeting $Cs_5Re_6S_8Br_7$ (as described above) was pulverized and stirred in 200 mL of 1 M aqueous HBr for 30 min. The mixture was filtered to give a small amount of red-brown solid and a bright yellow filtrate. Excess $(Bu_4N)Br$ (*ca*. 1.5 g) was added to the stirred filtrate which turned colorless upon formation of a yellow precipitate. The precipitate was collected by filtration and dissolved in 100 mL of acetonitrile to give an orange solution. Several drops of water and *ca*. 1 mL of $SOBr_2$ were added to the stirred solution, which underwent an immediate color change to red. The solution was reduced to dryness leaving a red solid which was recrystallized by evaporation from a *ca*. 1:1 (v:v) mixture of acetone and toluene. The resulting red plates were washed with successive 30-mL aliquots of toluene, water, toluene, and pentane and dried under vacuum to afford 2.44 g (71%) of pure product. Absorption spectrum (MeCN): $\lambda_{max}$ ($\epsilon_M$) 395 (sh, 2380), 492 (781), 541 (1270) nm. Anal. Calcd for $C_{48}H_{109}Br_6N_3S_8Re_6$: C, 22.33; H, 4.26; Br, 18.57; N, 1.63; Re, 43.28; S, 9.94. Found: C, 22.37; H, 4.31; Br, 18.88; N, 1.58; Re, 43.16; S, 9.79.

**$(Bu_4N)_4[Re_6S_8I_6]\cdot H_2O$.** A 1.12-g portion of the product recovered from a reaction targeting $Cs_6Re_6S_8I_8$ (as described above) was pulverized and stirred in 200 mL of 1 M aqueous HI for 2 h. The mixture was filtered to give a large amount of gray-black solid and a yellow filtrate. Solid KOH (30 g, 0.53 mol) was added to the filtrate and stirred until it completely dissolved. A 50-mL aliquot of 0.05 M aqueous $(Bu_4N)I$ was added to the stirred solution, which turned colorless upon formation of a yellow-orange precipitate. The precipitate was collected by filtration and dissolved in 100 mL of acetonitrile to give a yellow-orange solution. The solution was reduced to dryness leaving a yellow-orange solid that was crystallized by evaporation from a *ca*. 1:1 (v/v) mixture of acetone and toluene. The resulting yellow-orange plates were washed with successive 30-mL aliquots of toluene, water, toluene, and pentane to afford 0.041 g (4.3%) of product. Absorption spectrum (MeCN): $\lambda_{max}$ ($\epsilon_M$) 393 (sh, 3290), 420 (2200), 507 (sh, 755) nm.

**$(Bu_4N)_3[Re_6S_7(SH)I_6]\cdot 2Me_2CO$.** The product recovered (2.69 g) from a reaction targeting $Cs_6Re_6S_8I_8$ (as described above) was pulverized and stirred in 200 mL of 1 M aqueous $H_2SO_4$ for 1 h. The mixture was filtered to give a large amount of gray-black solid and a yellow-orange filtrate. A 50-mL aliquot of 0.05 M aqueous $(Bu_4N)I$ was added to the stirred filtrate which turned colorless upon formation of a brown precipitate. The precipitate was collected by filtration and dissolved in 100 mL of $CH_2Cl_2$ to give a red-brown solution. Three drops of concentrated aqueous $H_2SO_4$ were added, and the solution was stirred

**Table 3.** Crystallographic Data[a] for $Cs_5Re_6S_8Br_7$, $Cs_6Re_6S_8I_8$, $Cs_2Re_6Se_8Br_4$, $CsRe_6Se_8I_3$, and $Cs_4Re_6Se_8I_6$

| | $Cs_5Re_6S_8Br_7$ | $Cs_6Re_6S_8I_8$ | $Cs_2Re_6Se_8Br_4$ | $CsRe_6Se_8I_3$ | $Cs_4Re_6Se_8I_6$ |
|---|---|---|---|---|---|
| formula wt | 2597.6 | 3186.3 | 2334.3 | 2262.5 | 3041.9 |
| space group | $R\bar{3}c$ | $Fm\bar{3}m$ | $P2_1/n$ | $P2_1/n$ | $P2_1/c$ |
| $Z$ | 6 | 4 | 2 | 4 | 4 |
| $a$, Å | 9.957(2) | 15.842(2) | 6.544(3) | 6.565(2) | 10.099(3) |
| $b$, Å | | | 18.687(7) | 19.678(9) | 28.922(8) |
| $c$, Å | 54.55(2) | | 9.263(4) | 15.793(6) | 11.667(3) |
| $\beta$, deg | | | 104.26(3) | 96.77(3) | 106.27(2) |
| $V$, Å$^{-3}$ | 4685(2) | 3976(1) | 1098.0(8) | 2026(1) | 3271(2) |
| $d_{calc}$, g/cm$^3$ | 5.524 | 5.324 | 7.061 | 7.417 | 6.176 |
| $\mu$, mm$^{-1}$ | 38.39 | 30.24 | 56.73 | 56.39 | 41.06 |
| $R^b$ ($R_w^c$), % | 7.56 (7.96) | 5.39 (6.51) | 6.70 (6.81) | 7.64 (7.03) | 5.03 (4.99) |

[a] Obtained at 223 K with graphite monochromated Mo K$\alpha$ ($\lambda = 0.71073$ Å) radiation. [b] $R = \sum||F_o| - |F_c||/\sum|F_o|$. [c] $R_w = \{\sum[w(|F_o| - |F_c|)^2/\sum[w|F_o|^2]\}^{1/2}$.

**Table 4.** Crystallographic Data[a] for $(Bu_4N)_4[Re_6S_8Cl_6]$, $(Bu_4N)_3[Re_6S_7(SH)Cl_6]$, $(Bu_4N)_4[Re_6S_8Br_6]\cdot H_2O$, and $(Bu_4N)_3[Re_6S_7(SH)Br_6]\cdot 2Me_2CO$

| | $(Bu_4N)_4[Re_6S_8Cl_6]$ | $(Bu_4N)_3[Re_6S_7(SH)Cl_6]$ | $(Bu_4N)_6[Re_6S_8Br_6]\cdot H_2O$ | $(Bu_4N)_3[Re_6S_7(SH)Br_6]\cdot 2Me_2CO$ |
|---|---|---|---|---|
| formula | $C_{64}H_{144}Cl_6N_4Re_6S_8$ | $C_{48}H_{109}Cl_6N_3Re_6S_8$ | $C_{64}H_{146}Br_6N_4ORe_6S_8$ | $C_{54}H_{121}Br_6N_3O_2Re_6S_8$ |
| formula wt | 2556.2 | 2314.8 | 2841.0 | 2697.7 |
| space group | *Pbca* | $P\bar{1}$ | $P2_1/c$ | $P\bar{1}$ |
| $Z$ | 4 | 2 | 4 | 2 |
| $a$, Å | 22.738(5) | 12.445(5) | 22.055(7) | 13.957(5) |
| $b$, Å | 16.585(6) | 17.482(5) | 16.832(6) | 16.870(6) |
| $c$, Å | 23.524(9) | 18.190(6) | 24.482(10) | 18.552(8) |
| α, deg | | 95.98(2) | | 76.30(3) |
| $\beta$, deg | | 106.53(3) | 90.87(3) | 76.02(3) |
| $\gamma$, deg | | 103.67(3) | | 77.62(3) |
| $V$, Å$^3$ | 8871(5) | 3624(2) | 9088(5) | 4061(3) |
| $d_{calc}$, g/cm$^3$ | 1.914 | 2.121 | 2.076 | 2.206 |
| $\mu$, mm$^{-1}$ | 8.559 | 10.47 | 10.82 | 12.10 |
| $R$ ($R_w$),[b] % | 6.06 (6.38) | 5.03 (5.20) | 4.83 (5.13) | 6.00 (6.26) |

[a] Obtained at 223 K with graphite monochromated Mo K$\alpha$ ($\lambda = 0.71073$ Å) radiation. [b] For definitions *cf.* Table 3.

**Table 5.** Crystallographic Data[a] for $(Bu_4N)_4[Re_6S_8I_6]\cdot H_2O$, $(Bu_4N)_3[Re_6S_7(SH)I_6]\cdot 2Me_2CO$, and $(Bu_4N)_3[Re_6Se_7(SeH)I_6]\cdot 2Me_2CO$

| | $(Bu_4N)_4[Re_6S_8I_6]\cdot H_2O$ | $(Bu_4N)_3[Re_6S_7(SH)I_6]\cdot 2Me_2CO$ | $(Bu_4N)_3[Re_6Se_7(SeH)I_6]\cdot 2Me_2CO$ |
|---|---|---|---|
| formula | $C_{64}H_{146}I_6N_4ORe_6S_8$ | $C_{54}H_{121}I_6N_3O_2Re_6S_8$ | $C_{54}H_{121}I_6N_3O_2Re_6Se_8$ |
| formula wt | 3122.9 | 2921.5 | 3353.8 |
| space group | $P2_1/c$ | $C2/c$ | $C2/c$ |
| $Z$ | 4 | 4 | 4 |
| $a$, Å | 22.170(7) | 28.631(12) | 28.227(11) |
| $b$, Å | 17.326(5) | 21.380(8) | 21.940(9) |
| $c$, Å | 24.682(9) | 14.741(5) | 14.995(6) |
| $\beta$, deg | 91.73(3) | 108.57(3) | 105.22(3) |
| $V$, Å$^{-3}$ | 9477(5) | 8553(6) | 8961(6) |
| $d_{calc}$, g/cm$^3$ | 2.189 | 2.269 | 2.486 |
| $\mu$, mm$^{-1}$ | 9.800 | 10.85 | 13.42 |
| $R$ ($R_w$),[b] % | 8.42 (8.72) | 6.77 (5.69) | 6.78 (6.74) |

[a] Obtained at 223 K with graphite monochromated Mo K$\alpha$ ($\lambda = 0.71073$ Å) radiation. [b] For definitions *cf.* Table 3.

for 30 min. The solution was then reduced to dryness, leaving a red solid which was recrystallized by evaporation from a *ca.* 1:1 (v/v) mixture of acetone and toluene. The resulting black crystals were washed with successive 30-mL aliquots of toluene, water, toluene, and pentane to afford 0.22 g (11%) of product. Absorption spectrum (MeCN): $\lambda_{max}$ ($\epsilon_M$) 534 (590), 586 (sh, 353) nm.

**$(Bu_4N)_3[Re_6Se_7(SeH)I_6]\cdot 2Me_2CO$.** The product recovered (1.957 g) from a reaction targeting $Cs_4Re_6Se_8I_6$ (as described above) was pulverized and stirred in 200 mL of 1 M aqueous HI for 2 h. The mixture was filtered to give a small amount of brown-black solid and a bright red filtrate. A 50-mL aliquot of 0.05 M aqueous $(Bu_4N)I$ was added to the stirred filtrate which turned colorless upon formation of a brown precipitate. The precipitate was collected by filtration and dissolved in 100 mL of acetonitrile to give a red-brown solution. Ten drops of $SOCl_2$ were added, and the solution was stirred for 15 min. The solution was then reduced to dryness, leaving a brown-black solid which was crystallized by evaporation from a *ca.* 1:1 (v/v) mixture of acetone and toluene. The resulting black, block-shaped crystals were washed with successive 30-mL aliquots of toluene, water, toluene, and pentane to afford 1.31 g (63%) of product. Absorption spectrum (MeCN): $\lambda_{max}$ ($\epsilon_M$) 477 (sh, 2060), 525 (sh, 1180), 609 (1190) nm. Anal. Calcd for $C_{48}H_{109}I_6N_3Se_8Re_6$: C, 17.72; H, 3.38; I, 23.43; N, 1.29; Re, 34.51; Se, 19.67. Found: C, 17.96; H, 3.42; I, 23.60; N, 1.26; Re, 34.32; Se, 19.36.

**X-ray Data Collection and Reduction.** Structures were determined for the compounds listed in Tables 3−5. Single crystals were picked from the reaction products, coated with Apiezon L grease, and attached to glass fibers. The crystals were then transferred to a Nicolet R3m/V diffractometer and cooled in a dinitrogen stream to −50 °C. Lattice parameters were obtained from least-squares analysis of more than 30 carefully centered reflections. Decay corrections were based on the measured intensities of reflections monitored periodically throughout the course of data collection; none of the crystals showed significant decay. The raw intensity data were converted (including corrections for scan speed, background, and Lorentz and polarization effects) to structure factor amplitudes and their esd's using the program XDISK from the SHELXTL PLUS 4.21/V software package. An empirical absorption correction based on the observed variation in intensity of azimuthal ($\Psi$) scans was applied to each data set using the program XEMP. For $Cs_5Re_6S_8Br_7$, $Cs_6Re_6S_8I_8$, $Cs_2Re_6Se_8Br_4$, $CsRe_6Se_8I_3$, and $Cs_4Re_6Se_8I_4$, the absorption correction was improved by collecting excess data used to average equivalent reflections. Further details of the data collection are deposited as supporting information. Crystal data are collected in Tables 3−5.

**Structure Solution and Refinement.** Space group assignments were based on systematic absences, *E* statistics, and successful refinement of the structures. Structures were solved by direct methods (XS) with the aid of difference Fourier maps and were refined ($F_o > 6\sigma F_o$) with successive full-matrix least-squares cycles (XLS). The structure of $(Bu_4N)_3[Re_6S_7(SH)Br_6]\cdot 2Me_2CO$ was solved in space group $P1$ and the solution adapted for $P\bar{1}$. In the $(Bu_4N)_3[Re_6Se_7(SeH)I_6]\cdot 2Me_2CO$ structure, all non-hydrogen atoms were refined anisotropically with the exception of those comprising the two acetone solvate molecules. For all other structures, light atoms ($Z < 9$) were refined isotropically, and the other atoms were refined anisotropically. Hydrogen atoms were not included in the final refinements except for those associated with the cations in $(Bu_4N)_3[Re_6S_7(SH)Br_6]\cdot 2Me_2CO$ and $(Bu_4N)_3[Re_6Se_7(SeH)I_6]\cdot 2Me_2CO$. In these two cases, hydrogen atoms were fixed at ideal locations 0.96 Å from the bonded carbon atom and given a uniform value of $U_{iso}$. After the final cycle of refinement of each structure, all parameters had shifted by less than 1% of their esd, and the difference Fourier map showed no significant electron density. Because of the large amount of data from the 12 structures reported and the constant cluster structural motif, metric parameters are summarized as ranges and mean values. Complete listings of structural data are deposited as supporting information.

All of the compounds absorb X-rays heavily, particularly the denser solid phases which exhibit linear absorption coefficients $\mu$, of greater than 30 $mm^{-1}$ (see Table 3). For higher symmetry crystals, the empirical absorption correction proved adequate when combined with collection of excess data (generally, one half of the full sphere) used to average equivalent reflection intensities.

**Other Physical Measurements.** X-ray powder diffraction data were collected on a Scintag XDS-2000 diffractometer using Cu Kα radiation ($\lambda = 1.5406$ Å). Electron microprobe analyses were carried out with a Cameca MBX electron microprobe operating at 15 keV and 15 nA and employing a Tracor Northern TN-1310 wavelength-dispersive spectrometer. Absorption spectra were measured with a Cary Model 3 spectrophotometer. Cyclic voltammetry was performed with an EG&G Model 163 potentiostat, 0.1 M $(Bu_4N)(PF_6)$ supporting electrolyte, and a Pt disk working electrode. Potentials were determined vs an SCE reference electrode.

## Results and Discussion

**Solid-State Syntheses.** Solid-state reactions proceeded along lines typical of previous rhenium chalcohalide cluster phase preparations.[13,41] Stoichiometric amounts of elemental or binary compounds were intimately ground and reacted at high temperature (800, 850, or 900 °C) under non-oxidative conditions in sealed fused silica tubes. Crystal growth was promoted by slow cooling rates; various attempts at employing transport agents such as $I_2$ were unsuccessful. Reactants were situated at the cooler end of the tube to ensure contact with the cesium halide, which otherwise tended to migrate out of the reaction mixture. Reactions targeting $Cs_6Re_6S_8I_8$ were often contaminated by large amounts of an unidentified phase, but usually improved with addition of two extra equivalents of CsI to the reaction mixture. The XRPD pattern of this insoluble black impurity displayed extremely intense low-angle ($2\theta < 20°$) peaks characteristic of cluster-containing phases. Most likely, the impurity is some higher-dimensional product $Cs_nRe_6S_8I_{2+n}$ ($0 \le n < 4$); unfortunately, attempts at obtaining it in the form of sizable crystals failed. All other preparations were essentially quantitative, as monitored by XRPD.

(41) (a) Leduc, L.; Padiou, J.; Perrin, A.; Sergent, M. *J. Less-Common Met.* **1983**, *95*, 73. (b) Leduc, L.; Perrin, A.; Sergent, M. C. *R. Acad. Sci. Ser. 2* **1983**, *296*, 961. (c) Leduc, L.; Perrin, A.; Sergent, M.; Le Traon, F.; Pilet, J. C.; Le Traon, A. *Mater. Lett.* **1985**, *3*, 209.

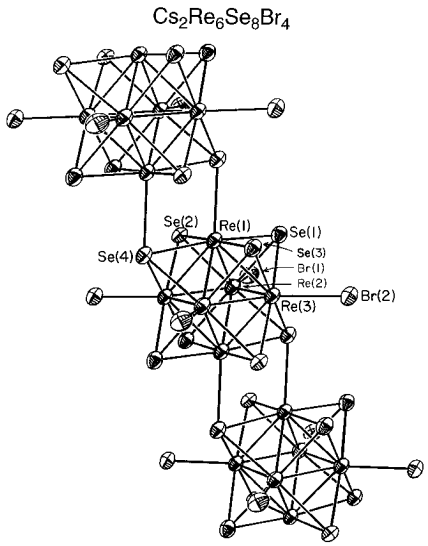


**Figure 6.** Local cluster environment in the structure of one-dimensional $Cs_2Re_6Se_8Br_4$; ellipsoids are drawn at the 50% probability level. Inversion centers are located at the center of each cluster and each $Re_2Se_2$ rhomb.

**Dimensional Reduction of $Re_6Se_8X_2$ (X = Cl, Br, "I").** A maximum of three distinct steps have been encountered in the dimensional reduction of $Re_6Se_8Cl_2$ (Figure 2), as observed with the incorporation of TlCl:[13]

$$\underset{\text{2-D}}{Re_6Se_8Cl_2} \xrightarrow{TlCl} \underset{\text{2-D}}{TlRe_6Se_8Cl_3} \xrightarrow{TlCl} \underset{\text{1-D}}{Tl_2Re_6Se_8Cl_4} \xrightarrow{3TlCl} \underset{\text{0-D}}{Tl_5Re_6Se_8Cl_7} \quad (6)$$

(Again, it should be emphasized that dimensional reduction equations such as eq 6 are intended to convey the formalistic relationship between structures, and not necessarily a specific synthetic pathway.) The first step involves uptake of a single equivalent of TlCl to yield $TlRe_6Se_8Cl_3$. Here the overall dimensionality of the cluster framework has not been reduced; however, the rigidity of the sheets has relaxed substantially. Each $[Re_6Se_8]^{2+}$ core now has three associated terminal chlorides (*fac* arrangement) and three rhombic $Re_2Se_2$ interactions with neighboring cores, resulting in a dimpled, six-connected $[Re_6Se_8Cl_3]^{1-}$ framework. Addition of one more equivalent of TlCl gives rise to $Tl_2Re_6Se_8Cl_4$, wherein the dimensionality and connectedness of the framework have now been reduced to one and four, respectively. The chain structure of this phase matches that of $Cs_2Re_6Se_8Br_4$ (Figure 6) described below and is derived from $Re_6Se_8Cl_2$ by simply terminating the core−core linkages in one dimension. The terminus in the dimensional reduction of $Re_6Se_8Cl_2$ is gained with incorporation of five total equivalents to TlCl to form zero-dimensional $Tl_5Re_6Se_8Cl_7$, which is isotypic with the $Cs_5Re_6S_8Br_7$ (see Figure 9, below) structure and features the molecular cluster $[Re_6Se_8Cl_6]^{4-}$. While $TlRe_6Se_8Cl_3$ forms quantitatively, the two lower-dimensional phases $Tl_2Re_6Se_8Cl_4$ and $Tl_5Re_6Se_8Cl_7$ are consistently produced only in negligible overall yields. Further, the strong interactions of $Tl^+$ cations with the clusters render all of these compounds insoluble. Thus, while the preceding phases establish the potential of the dimensional reduction approach in dismantling the $Re_6Se_8Cl_2$ framework, they do not accomplish our ultimate goal of providing the $[Re_6Se_8]^{2+}$ core in *soluble* molecular form.

**Table 6.** Selected Interatomic Distances (Å) and Angles (deg) for $Tl_2Re_6S_8Cl_4$, $Tl_2Re_6Se_8Cl_4$, and $Cs_2Re_6Se_8Br_4$

| | $Tl_2Re_6S_8Cl_4$[a] | $Tl_2Re_6Se_8Cl_4$[a] | $Cs_2Re_6Se_8Br_4$ |
|---|---|---|---|
| Re−Re | 2.590(5)−2.634(5) | 2.618(3)−2.666(3) | 2.605(3)−2.662(3) |
| mean | 2.603(11) | 2.63(2) | 2.62(2) |
| Re···Re[b] | 3.216−3.259 | 3.407 | 3.370 |
| mean | 3.24(2) | | |
| Re−Q[c] | 2.35(3)−2.45(3) | 2.500(7)−2.517(6) | 2.506(6)−2.527(5) |
| mean | 2.40(3) | 2.510(5) | 2.515(7) |
| Re−Q[b] | 2.49(3)−2.56(2) | 2.600(7)−2.633(5) | 2.617(5)−2.638(6) |
| mean | 2.51(3) | 2.62(2) | 2.63(1) |
| Re−X | 2.38(2)−2.44(3) | 2.411(12)−2.414(11) | 2.543(7)−2.573(6) |
| mean | 2.41(2) | 2.413(2) | 2.56(2) |
| Re−Re−Re[d] | 59.5(1)−60.9(1) | 59.4(1)−60.9(1) | 59.3(1)−61.0(1) |
| Re−Re−Re[e] | 89.4(2)−90.6(2) | 89.3(1)−90.7(1) | 89.4(1)−90.6(1) |
| Re−Re−X | 133.2(6)−137.5(5) | 134.1(4)−136.4(4) | 131.2(2)−138.8(2) |
| mean | 135(1) | 135.2(7) | 135(2) |
| Re−Q−Re[c] | 63.7(5)−66.7(6) | 61.2(1)−64.1(2) | 62.1(1)−64.0(1) |
| mean | 65(1) | 63.0(8) | 62.6(9) |
| Q−Re−Q[b] | 99.6(7)−100.0(6) | 98.7(2) | 100.2(2) |
| mean | 99.8(2) | | |
| Q−Re−X | 90.4(8)−95.6(8) | 89.7(4)−93.4(4) | 89.4(1)−95.2(2) |
| mean | 93(2) | 92.2(6) | 92(2) |

[a] Reference 15. [b] Within core-linking $Re_2Q_2$ rhombs. [c] Excluding $Re_2Q_2$ rhombs. [d] Within triangular faces. [e] Within equatorial squares.

Toward this end, attempts were made at utilizing the cesium halides as dimensional reduction agents.[42] Uptake of cesium chloride and cesium bromide is limited to a single step:

$$\underset{\text{2/3-D}}{Re_6Se_8X_2} \xrightarrow{2CsX} \underset{\text{1-D}}{Cs_2Re_6Se_8X_4} \qquad (X = Cl, Br) \qquad (7)$$

The structure of $Cs_2Re_6Se_8Br_4$ (isomorphous with $Cs_2Re_6Se_8Cl_4$)[13] exhibits one-dimensional chains composed of $[Re_6Se_8]^{2+}$ cores linked by $Re_2Se_2$ rhombs at *trans* rhenium apices, as shown in Figure 6. The chains are sheathed with terminal bromides, which ligate the remaining four rhenium atoms of each cluster core to afford the connectivity $Cs_2[Re_6Se^i{}_6Se^{i\text{-}a}{}_{2/2}]Se^{a\text{-}i}{}_{2/2}Br^a{}_4$. Nearly identical chains are present in the $Re_6Se_8Br_2$ parent (isotypic with $Re_6S_8Cl_2$, Figure 4) wherein each is linked to four neighboring chains via bridging bromide atoms. Thus, the inclusion of CsBr terminates all of the bromide bridges, and opens up the structure by inserting $Cs^+$ cations[43] between chains, effectively reducing the framework connectedness to four and the dimensionality to one. Interatomic distances and angles for the chains in $Cs_2Re_6Se_8Br_4$ are summarized in Table 6, and except for marginally shorter Re−Br distances, bear no significant differences from those in $Re_6Se_8Br_2$.[10a] In both structures, the $[Re_6Se_8]^{2+}$ core consists of a regular $Re_6$ octahedron concentric with an $Se_8$ cube; the regularity of the latter is disrupted somewhat by the slightly (*ca.* 0.1 Å) longer Re−Se bonds within core-linking $Re_2Se_2$ rhombs. This last observation holds true for all frameworks featuring $[Re_6Q_8]^{2+}$ (Q = S, Se) cores linked in such a manner. Despite containing frameworks with a connectedness of just four, the compactness of their $Re_2Se_2$ core-linking interactions prevents $Cs_2Re_6Se_8X_4$ (X = Cl, Br) from breaking up into discrete clusters under standard excision conditions.[44] Interestingly, none of the above $M^I{}_2Re_6Se_8X_4$ phases assume the isomeric two-dimensional cluster framework of Figure 1, as adopted by $Re_6Se_6Cl_6$.[3]

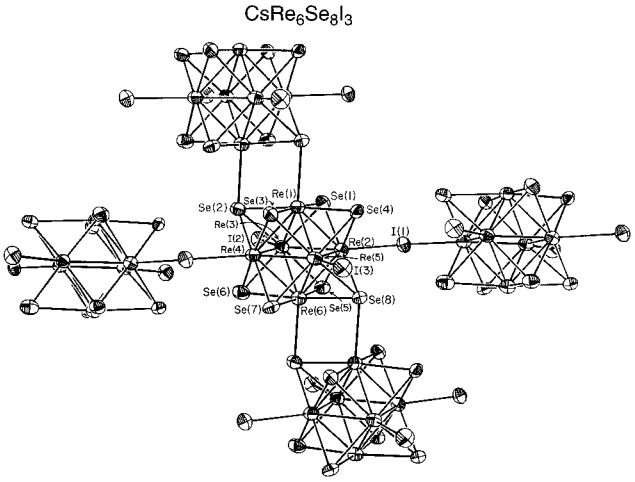


**Figure 7.** Local cluster environment in the structure of two-dimensional $CsRe_6Se_8I_3$ (=$Cs[Re_6Se^i{}_6Se^{i\text{-}a}{}_{2/2}]Se^{a\text{-}i}{}_{2/2}I^a{}_2I^{a\text{-}a}{}_{2/2}$); ellipsoids are drawn at the 50% probability level. Selected mean interatomic distances (Å) and angles (deg) are as follows: Re−Re 2.63(2), non-rhomb Re−Se 2.51(1), bridging Re−I 2.819(1), terminal Re−I 2.757(3), Re−Re−Re 60.0(6) and 90.0(6), Re−Re−I 135(2), Re−$Se^i$−Re 62.9(8), Re−I−Re 119.1; within $Re_2Se_2$ rhombs Re−Se 2.603(2), Re···Re 3.390, Se−Re−Se 98.7.

Dimensional reduction of the fictitious $Re_6Se_8I_2$ parent solid with CsI proceeds in two steps:

$$\underset{\text{?-D}}{\text{“}Re_6Se_8I_2\text{”}} \xrightarrow{CsI} \underset{\text{2-D}}{CsRe_6Se_8I_3} \xrightarrow{3CsI} \underset{\text{0-D}}{Cs_4Re_6Se_8I_6} \qquad (8)$$

The structure of the two-dimensional phase $CsRe_6Se_8I_3$ (Figure 7) is built up from $[Re_6Se_8]^{2+}$ cores linked in one dimension via *trans* rhombic $Re_2Se_2$ interactions and in another through *trans* bridging iodide ligands, with the remaining two apices capped by terminal iodides. The resulting six-connected sheet is readily obtained from the $Re_6S_8Cl_2$ structure (Figure 4) by terminating halide bridges in one dimension. Interatomic

(42) Halides of the smaller alkali metals were found to be considerably less effective in this role.

(43) The $Cs^+$ cations in all of the new phases display a complex coordination environment (with coordination number ≥7, and a geometry often defying simple description) involving both chalcogenide and halide atoms.

(44) Given the apparent rigidity of the chains in these compounds, an intriguing alternative to excision is direct dissolution of entire one-dimensional $[Re_6Se_8X_4]^{2-}$ chains. Precedence for such a seemingly improbable occurrence has been established with the $[Mo_6Q_6]^{2-}$ (Q = Se, Te) chains in $A_2Mo_6Q_6$ (A = Li, K), which dissolve intact in highly polar solvents like DMSO: Tarascon, J. M.; DiSalvo, F. J.; Chen, C. H.; Carroll, P. J.; Walsh, M.; Rupp, L. *J. Solid State Chem.* **1985**, *58*, 290.

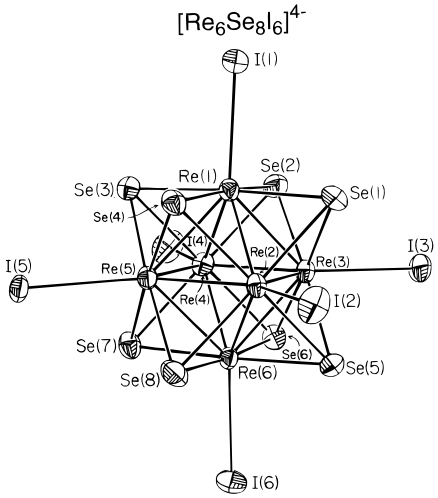


**Figure 8.** Structure of the discrete $[Re_6Se_8I_6]^{4-}$ clusters in $Cs_4Re_6Se_8I_6$ (60% probability ellipsoids).

distances and angles are summarized in the legend of Figure 7; again, there is some variation in the Re−Se and Re−I bond lengths, depending upon whether or not the Se or I atom is involved in intercore bonding. Note that the $CsRe_6Se_8I_3$ structure is an isomeric alternative to the $TlRe_6Se_8Cl_3$ structure described above. A soluble molecular form of the $[Re_6Se_8]^{2+}$ core is realized with incorporation of four total equivalents of CsI in the phase $Cs_4Re_6Se_8I_6$. Here, all of the linkages between clusters have been replaced by terminal iodide atoms, resulting in completely isolated $[Re_6Se_8I_6]^{4-}$ clusters, as shown in Figure 8. Relevant distances and angles are listed in Table 7. The absence of any $Re_2Se_2$ core-linking interactions enables the cluster core to relax into a more uniform geometry, closely approaching $O_h$ symmetry. However, this symmetry is somewhat disrupted by the terminal iodide ligands, which lie slightly and irregularly displaced from their ideal positions along the 4-fold rotational axes (as is apparent in Figure 8). The mean Re−Re distance of 2.625(5) Å is comparable to that observed in the other $[Re_6Se_8]^{2+}$ core-containing phases, and corresponds to a Re−Re single bond, as expected for an $M_6Q_8$ cluster with an ideal configuration of 24 metal-based electrons.[45] Comparison with the $[Re_6Se_8Cl_6]^{4-}$ cluster in $Tl_5Re_6Se_8Cl_7$ (Table 7) exposes no obvious core differences.

**Dimensional Reduction of $Re_6S_8X_2$ (X = Cl, Br, "I").** Dimensional reduction of the three-dimensional parent phase $Re_6S_8Cl_2$ (Figure 4) with TlCl has been demonstrated to progress in two steps:[13]

$$\underset{\text{3-D}}{Re_6S_8Cl_2} \xrightarrow{2TlCl} \underset{\text{1-D}}{Tl_2Re_6S_8Cl_4} \xrightarrow{3TlCl} \underset{\text{0-D}}{Tl_5Re_6S_8Cl_7} \qquad (9)$$

Obtained in near quantitative yields, the dimensionally-reduced phases are structurally analogous to their Se-containing counterparts, $Tl_2Re_6Se_8Cl_4$ and $Tl_5Re_6Se_8Cl_7$, described above. Geometric parameters for $Tl_2Re_6S_8Cl_4$ and $Tl_2Re_6Se_8Cl_4$ are collected in Table 6 for comparison. The only remarkable differences between the two structures arise as a result of the shorter Re−S bonds (mean of 2.40(3) Å versus 2.510(5) Å for Re−Se), which induce contraction of both core $S_8$ cubes and $Re_2S_2$ rhombs, bringing cluster cores within chains closer together.

Again, cesium halides are the reagents of choice for directly preparing soluble molecular $[Re_6S_8]^{2+}$ core-containing phases via dimensional reduction. The three-dimensional $Re_6S_8X_2$ (X = Cl, Br) parent frameworks are completely dismantled with incorporation of 5 equiv of CsX; no intermediate phases with fewer equivalents of CsX were targeted or encountered.

$$\underset{\text{3-D}}{Re_6S_8X_2} \xrightarrow{5CsX} \underset{\text{0-D}}{Cs_5Re_6S_8X_7} \qquad (X = Cl, Br) \qquad (10)$$

The structure of the discrete $[Re_6S_8Br_6]^{4-}$ cluster in $Cs_5Re_6S_8Br_7$ is depicted in Figure 9. Both $Cs_5Re_6S_8Cl_7$ and $Cs_5Re_6S_8Br_7$ are isotypic with $Tl_5Re_6Q_8Cl_7$ (Q = S, Se). The extra equivalent of $M^IX$ in these $M^I_5Re_6Q_8X_7$ (=$M^I_4[Re_6Q_8X_6]\cdot M^IX$) phases presumably facilitates the packing of clusters in the crystal lattice. Dimensional reduction of the fictitious parent $Re_6S_8I_2$ also terminates with a molecular product; insoluble intermediate phases were possibly observed by XRPD (*vide supra*), but could not be structurally characterized.

$$\underset{\text{?-D}}{\text{“}Re_6S_8I_2\text{”}} \xrightarrow{6CsI} \underset{\text{0-D}}{Cs_6Re_6S_8I_8} \qquad (11)$$

Two adventitious equivalents of CsI are present in $Cs_6Re_6S_8I_8$ (=$Cs_4[Re_6S_8I_6]\cdot 2CsI$) which crystallizes in the cubic space group $Fm\bar{3}m$. Pleasingly, the symmetry of the crystal lends itself to the cluster imposing it with perfect $O_h$ symmetry. Interatomic distances and angles for the molecular $[Re_6S_8X_6]^{4-}$ (X = Cl, Br, I) clusters in these Cs-containing phases are summarized in Table 8. Other than the expected increase in Re−X bond distance with increasing halide radius, the clusters do not exhibit any statistically meaningful geometric differences. A comparison of $[Re_6S_8X_6]^{4-}$ and $[Re_6Se_8X_6]^{4-}$ (X = Cl, I; Tables 7 and 8) reveals that the expected differences due to the longer Re−Se bonds are accompanied by a subtle isotropic expansion of the $Re_6$ octahedron.

**Enumeration of $[M_6Q_8]$ Framework Connectivities.** The $Re_6Q_8Cl_2$ (Q = S, Se) parent frameworks and their dimensionally reduced offspring all share a number of defining attributes. All are composed of $[Re_6Q_8]^{2+}$ core units with six Re apices capped by one of three different types of outer ligands: a Q atom internal to a neighboring core ($Q^{a\text{-}i}$), a bridging halide atom linking it to the apex of a neighboring core ($X^{a\text{-}a}$), or a terminal halide atom ($X^a$). Furthermore, in a given framework, all cores display an identical coordination environment. Under these constraints, it is a simple matter to enumerate the possible framework connectivities. A compilation of the 28 possibilities for general $[M_6Q_8]$ cluster frameworks is set forth in Table 9, along with some structurally proven examples.[3,6,8,10,13,36,37,46−49] As one scans the table from top to bottom, the connectedness of the framework decreases from a maximum of 12 (with each core engaged in six rhombic $M_2Q_2$ linkages) down to 0. The

(45) Mingos, D. M. P.; Wales, D. J. *Introduction to Cluster Chemistry*; Prentice Hall: Englewood Cliffs, NJ, 1990; pp 286−290 and references therein.

(46) (a) Potel, M.; Gougeon, P.; Chevrel, R.; Sergent, M. *Rev. Chim. Mineral.* **1984**, *21*, 509. (b) Bars, O.; Guillevic, J.; Grandjean, D. *J. Solid State Chem.* **1973**, *6*, 48. (c) Guillevic, J.; Lestrat, H.; Grandjean, D. *Acta Crystallogr.* **1976**, *B32*, 1342. (d) Perrin, C.; Chevrel, R.; Sergent, M. *Mater. Res. Bull.* **1979**, *14*, 1505.

(47) (a) Perrin, C.; Sergent, M.; Le Traon, F.; Le Traon, A. *J. Solid State Chem.* **1978**, *25*, 197. (b) Bateman, I. R.; Blount, J. F.; Dahl, L. F. *J. Am. Chem. Soc.* **1966**, *88*, 1082. (c) Simon, A.; von Schnering, H. G.; Schäfer, H. *Z. Anorg. Allg. Chem.* **1967**, *355*. 295. (d) Imoto, H.; Corbett, J. D. *Inorg. Chem.* **1980**, *19*, 1241.

(48) Franolic, J. D.; Long, J. R.; Holm, R. H. *J. Am. Chem. Soc.* **1995**, *117*, 8139.

(49) (a) Perrin, A.; Leduc, L.; Potel, M.; Sergent, M. *Mater. Res. Bull.* **1990**, *25*, 1227. (b) Fedorov, V. E.; Mishchenko, A. V.; Kolesov, B. A.; Gubin, S. P.; Slovokhotov, Y. L.; Struckhov, Y. T. *Soviet. J. Coord. Chem.* **1985**, *11*, 980. (c) Leduc, L.; Perrin, A.; Sergent, M.; Le Traon, F.; Pilet, J. C.; Le Traon, A. *Mater. Lett.* **1985**, *3*, 209.

**Table 7.** Selected Interatomic Distances (Å) and Angles (deg) for $Tl_5Re_6Se_8Cl_7$, $Cs_4Re_6Se_8I_6$, and $[Re_6Se_7(SeH)I_6]^{3-}$

| | $Tl_5Re_6Se_8Cl_7$[a] | $Cs_4Re_6Se_8I_6$ | $[Re_6Se_7(SeH)I_6]^{3-}$[b] |
|---|---|---|---|
| Re−Re | 2.609(2)−2.619(2) | 2.617(4)−2.635(4) | 2.616(2)−2.632(2) |
| mean | 2.614(5) | 2.625(5) | 2.624(6) |
| Re−Se | 2.520(4)−2.526(3) | 2.505(6)−2.534(7) | 2.494(3)−2.515(3) |
| mean | 2.523(3) | 2.519(7) | 2.506(5) |
| Re−X | 2.431(8) | 2.779(5)−2.801(5) | 2.768(3)−2.777(3) |
| mean | | 2.793(8) | 2.773(4) |
| Re−Re−Re[c] | 59.7(1)−60.1(1) | 59.7(1)−60.4(1) | 59.7(1)−60.3(1) |
| mean | 60.0(2) | 60.0(2) | 60.0(2) |
| Re−Re−Re[d] | 90.0(1) | 89.7(1)−90.2(1) | 89.5(1)−90.5(1) |
| mean | | 90.0(2) | 90.0(4) |
| Re−Re−Se | 58.7(1)−59.0(1) | 58.1(2)−58.9(2) | 58.0(1)−58.8(1) |
| mean | 58.8(1) | 58.6(2) | 58.4(2) |
| Re−Re−X | 133.4(2)−136.6(2) | 131.1(1)−139.0(1) | 133.6(1)−136.8(1) |
| mean | 135(1) | 135(2) | 135(1) |
| Re−Se−Re | 62.3(1)−62.5(1) | 62.4(2)−63.1(2) | 62.9(1)−63.5(1) |
| mean | 62.4(1) | 62.8(2) | 63.1(2) |
| Se−Re−Se | 89.7(1)−90.2(1) | 89.1(2)−90.8(2) | 89.4(1)−90.5(1) |
| mean | 90.0(2) | 89.9(5) | 89.9(3) |
| Se−Re−X | 90.7(2)−92.8(2) | 87.1(2)−96.2(2) | 90.1(1)−93.7(1) |
| mean | 91(1) | 92(2) | 92(1) |

[a] Reference 13. [b] From $(Bu_4N)_3[Re_6Se_7(SeH)I_6]\cdot 2Me_2CO$. [c] Within triangular faces. [d] Within equatorial squares.

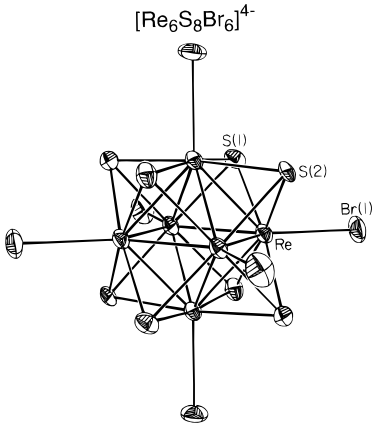


**Figure 9.** Structure of the discrete $[Re_6S_8Br_6]^{4-}$ cluster in $Cs_5Re_6S_8Br_7$ (50% probability ellipsoids). The cluster resides on a $\bar{3}$ symmetry site, with atom S(2) on the 3-fold rotation axis.

**Table 8.** Selected Interatomic Distances (Å) and Angles (deg) for $Cs_5Re_6S_8Cl_7$, $Cs_5Re_6S_8Br_7$, and $Cs_6Re_6S_8I_8$

| | $Cs_5Re_6S_8Cl_7$ | $Cs_5Re_6S_8Br_7$ | $Cs_6Re_6S_8I_8$ |
|---|---|---|---|
| Re−Re | 2.594(2)−2.559(2) | 2.593(3)−2.599(2) | 2.607(3) |
| mean | 2.597(3) | 2.596(3) | |
| Re−S | 2.395(6)−2.404(10) | 2.380(12)−2.407(13) | 2.408(11) |
| mean | 2.399(3) | 2.397(10) | |
| Re−X | 2.421(10) | 2.596(6) | 2.780(5) |
| Re−Re−Re[a] | 59.9(1)−60.1(1) | 59.9(1)−60.1(1) | 60.0(1) |
| mean | 60.0(1) | 60.0(1) | |
| Re−Re−Re[b] | 90.0(1) | 90.0(1) | 90.0(1) |
| Re−Re−S | 57.1(2)−57.3(1) | 56.7(3)−57.6(2) | 57.2(2) |
| mean | 57.2(1) | 57.2(3) | |
| Re−Re−X | 133.8(2)−136.2(2) | 133.5(2)−136.5(1) | 135.0(1) |
| mean | 135.0(9) | 135(1) | |
| Re−S−Re | 63.3(3)−65.7(2) | 65.3(4)−65.8(3) | 65.6(4) |
| mean | 65.5(1) | 65.6(2) | |
| S−Re−S | 89.7(2)−89.9(2) | 89.4(3)−90.2(3) | 89.8(1) |
| mean | 89.8(1) | 89.8(3) | |
| S−Re−X | 92.3(3)−94.6(2) | 92.1(3)−94.8(2) | 93.4(2) |
| mean | 93.4(9) | 93(1) | |

[a] Within triangular faces. [b] Within equatorial squares.

corresponding trend in the dimensionality of structured examples is much less unwavering.[50]

Excluding the two end points $M_6Q_8$ and $M_6Q_8X_6$, all of the stoichiometries in Table 9 have at least two possible connectivity formulations available. From the list of examples, we see that in three cases ($M_6Q_8X_2$, $M_6Q_8X_3$, and $M_6Q_8X_4$) more than one of these structural isomers has been realized experimentally. What drives a cluster framework to choose one connectivity over another? The present work may help shed some light on this difficult issue. Cluster systems in which all eight of the core Q atoms are chalcogenides display a pronounced tendency to form rhombic $M_2Q_2$ connections directly between cores. On the other hand, systems with eight halide atoms in the core never employ this connectivity mode, relying strictly upon outer halide bridges.[51] Apparently, the negative charge of a chalcogenide atom is sufficient (or even prefers) to support a $\mu_4$ bridging environment with four surrounding, positively-charged metal centers, whereas the lesser negative charge of a halide atom is not. The absence of direct core linkages in mixed-core phases of the type $Re_6Q_{8-n}X_{2+2n}$ (Q = S, Se; X = Cl, Br; $n$ = 1, 2, 3, 4) is perhaps attributable to the ease of disorder of the core anions, due to their similarity in size. Finally, among phases of the type $M^I_nRe_6Q_8X_{2+n}$ ($M^I$ = Cs, Tl; Q = S, Se; X = Cl, Br, I; $n$ = 0, 1, 2, 4, 5, 6), there exists an occasional preference of the softer halides for bridging ($X^{a\text{-}a}$) over terminal ($X^a$) ligand roles. Instances of such behavior are evident in the structures of $Re_6Se_8Cl_2$ and $Re_6Q_8Br_2$, as well as $TlRe_6Se_8Cl_3$ and $CsRe_6Se_8I_3$.

**Solution Chemistry.** Successful demonstration of the dimensional reduction of $Re_6S_8Cl_2$ and $Re_6Se_8Cl_2$ type frameworks is punctuated by the establishment of their solution-phase analogues. The compounds $Cs_5Re_6S_8X_7$ (X = Cl, Br) and $Cs_6Re_6S_8I_8$ readily dissolve in aqueous acid to give a bright yellow or yellow-orange solution. The solutions are made alkaline to prevent core protonation (*vide infra*), and the clusters precipitated by addition of excess $(Bu_4N)X$ (X = Cl, Br, I). The solids, which are highly soluble in acetonitrile and dichloromethane, are collected from the filtration apparatus by dissolution in acetonitrile and reduction to dryness. Recrystallization from a mixture of acetone and toluene affords the soluble molecular products $(Bu_4N)_4[Re_6S_8Cl_6]$, $(Bu_4N)_4[Re_6S_8Br_6]\cdot H_2O$, and $(Bu_4N)_4[Re_6S_8I_6]\cdot H_2O$. The crystal structures of these products confirm retention of the $[Re_6S_8X_6]^{4-}$ cluster in solution.

(50) Note that, for reasons analogous to those explained above for simple metal−anion frameworks, the connectivity formulation dictates the connectedness, but *not* the dimensionality, of the cluster framework.

(51) This observation is true only of $[M_6X_8]$ cluster frameworks, and does not extend to $[M_6X_{12}]$ cluster systems in which the core halides are edge-bridging ($\mu_2$).

**Table 9.** Possible Connectivities for $[M_6Q_8]$ Cluster Frameworks and Some Structurally Proven Examples

| formula | framework connectivity | conn[a] | examples[b] | ref |
|---|---|---|---|---|
| $M_6Q_8$ | $[M_6Q^i{}_2Q^{i\text{-}a}{}_{6/2}]Q^{a\text{-}i}{}_{6/2}$ | 12 | $Mo_6Q_8$, $PbMo_6Se_8$, $Mo_6S_6Br_2$ (3-D) | 46 |
| $M_{12}Q_{16}X$ | $[M_6Q^i{}_3Q^{i\text{-}a}{}_{5/2}]Q^{a\text{-}i}{}_{5/2}X^{a\text{-}a}{}_{1/2}$ | 11 | | |
| $M_6Q_8X$ | $[M_6Q^i{}_3Q^{i\text{-}a}{}_{5/2}]Q^{a\text{-}i}{}_{5/2}X^a$ | 10 | | |
| | $[M_6Q^i{}_4Q^{i\text{-}a}{}_{4/2}]Q^{a\text{-}i}{}_{4/2}X^{a\text{-}a}{}_{2/2}$ | 10 | | |
| $M_{12}Q_{16}X_3$ | $[M_6Q^i{}_4Q^{i\text{-}a}{}_{4/2}]Q^{a\text{-}i}{}_{4/2}X^aX^{a\text{-}a}{}_{1/2}$ | 9 | | |
| | $[M_6Q^i{}_5Q^{i\text{-}a}{}_{3/2}]Q^{a\text{-}i}{}_{3/2}X^{a\text{-}a}{}_{3/2}$ | 9 | | |
| $M_6Q_8X_2$ | $[M_6Q^i{}_4Q^{i\text{-}a}{}_{4/2}]Q^{a\text{-}i}{}_{4/2}X^a{}_2$ | 8 | $Re_6Se_8Cl_2$ (2-D) | 6 |
| | $[M_6Q^i{}_5Q^{i\text{-}a}{}_{3/2}]Q^{a\text{-}i}{}_{3/2}X^aX^{a\text{-}a}{}_{2/2}$ | 8 | | |
| | $[M_6Q^i{}_6Q^{i\text{-}a}{}_{2/2}]Q^{a\text{-}i}{}_{2/2}X^{a\text{-}a}{}_{4/2}$ | 8 | $Re_6S_8X_2$, $Re_6Se_8Br_2$ (3-D) | 10 |
| $M_{12}Q_{16}X_5$ | $[M_6Q^i{}_5Q^{i\text{-}a}{}_{3/2}]Q^{a\text{-}i}{}_{3/2}X^a{}_2X^{a\text{-}a}{}_{1/2}$ | 7 | | |
| | $[M_6Q^i{}_6Q^{i\text{-}a}{}_{2/2}]Q^{a\text{-}i}{}_{2/2}X^aX^{a\text{-}a}{}_{3/2}$ | 7 | | |
| | $[M_6Q^i{}_uQ^{i\text{-}a}{}_{1/2}]Q^{a\text{-}i}{}_{1/2}X^{a\text{-}a}{}_{5/2}$ | 7 | | |
| $M_6Q_8X_3$ | $[M_6Q^i{}_5Q^{i\text{-}a}{}_{3/2}]Q^{a\text{-}i}{}_{3/2}X^a{}_3$ | 6 | $TlRe_6Se_8Cl_3$ (2-D) | 13 |
| | $[M_6Q^i{}_6Q^{i\text{-}a}{}_{2/2}]Q^{a\text{-}i}{}_{2/2}X^a{}_2X^{a\text{-}a}{}_{2/2}$ | 6 | $CsRe_6Se_8I_3$ (2-D) | |
| | $[M_6Q^i{}_7Q^{i\text{-}a}{}_{1/2}]Q^{a\text{-}i}{}_{1/2}X^aX^{a\text{-}a}{}_{4/2}$ | 6 | | |
| | $[M_6Q^i{}_8]X^{a\text{-}a}{}_{6/2}$ | 6 | $Li_4Re_6S_{11}$, $Re_6Q_7Br_4$,[c] $Mo_6SeCl_{10}$, $Nb_6I_{11}$, $CsNb_6I_{11}$ (3-D) | 3, 37a, 47 |
| $M_{12}Q_{16}X_7$ | $[M_6Q^i{}_6Q^{i\text{-}a}{}_{2/2}]Q^{a\text{-}i}{}_{2/2}X^a{}_3X^{a\text{-}a}{}_{1/2}$ | 5 | | |
| | $[M_6Q^i{}_7Q^{i\text{-}a}{}_{1/2}]Q^{a\text{-}i}{}_{1/2}X^a{}_2X^{a\text{-}a}{}_{3/2}$ | 5 | | |
| | $[M_6Q^i{}_8]X^aX^{a\text{-}a}{}_{5/2}$ | 5 | | |
| $M_6Q_8X_4$ | $[M_6Q^i{}_6Q^{i\text{-}a}{}_{2/2}]Q^{a\text{-}i}{}_{2/2}X^a{}_4$ | 4 | $Tl_2Re_6Q_8Cl_4$, $Cs_2Re_6Se_8X_4$ (1-D) | 13 |
| | $[M_6Q^i{}_7Q^{i\text{-}a}{}_{1/2}]Q^{a\text{-}i}{}_{1/2}X^a{}_3X^{a\text{-}a}{}_{2/2}$ | 4 | | |
| | $[M_6Q^i{}_8]X^a{}_2X^{a\text{-}a}{}_{4/2}$ | 4 | $Re_6Se_6Cl_6$, $Mo_6Cl_{12}$,$W_6I_{12}$ (2-D) | 3, 36a, 48 |
| $M_{12}Q_{16}X_9$ | $[M_6Q^i{}_7Q^{i\text{-}a}{}_{1/2}]Q^{a\text{-}i}{}_{1/2}X^a{}_4X^{a\text{-}a}{}_{1/2}$ | 3 | | |
| | $[M_6Q^i{}_8]X^a{}_3X^{a\text{-}a}{}_{3/2}$ | 3 | | |
| $M_6Q_8X_5$ | $[M_6Q^i{}_7Q^{i\text{-}a}{}_{1/2}]Q^{a\text{-}i}{}_{1/2}X^a{}_5$ | 2 | | |
| | $[M_6Q^i{}_8]X^a{}_4X^{a\text{-}a}{}_{2/2}$ | 2 | $Re_6S_5Cl_8$, $NaMo_6Cl_{13}$ (1-D) | 8a, 36b |
| $M_{12}Q_{16}X_{11}$ | $[M_6Q^i{}_8]X^a{}_5X^{a\text{-}a}{}_{1/2}$ | 1 | | |
| $M_6Q_8X_6$ | $[M_6Q^i{}_b]X^a{}_6$ | 0 | $Tl_5Re_6Q_8Cl_7$, $Cs_5Re_6S_8X_7$, $Cs_6Re_6S_8I_8$, $Cs_4Re_6Se_8I_6$, $Re_6Q_4Cl_{10}$, $KRe_6Se_5Cl_9$, $RbRe_6S_5Cl_9$, $A_{10}M_6S_{14}$,[d] $PbMo_6X_{14}$[e] (0-D) | 8b, 13, 36c, 37b, 49 |

[a] Framework connectedness. [b] Q = S, Se; X = Cl, Br. [c] Complete structural details have not been published. [d] A = Rb, Cs; M = Tc, Re. [e] X = Cl, Br, I.

**Table 10.** Selected Interatomic Distances (Å) and Angles (deg) for $[Re_6S_8X_6]^{4-}$ (X = Cl, Br, I)

| | $[Re_6S_8Cl_6]^{4-}$ [a] | $[Re_6S_8Br_6]^{4-}$ [b] | $[Re_6S_8I_6]^{4-}$ [c] |
|---|---|---|---|
| Re−Re | 2.597(2)−2.609(2) | 2.583(3)−2.608(3) | 2.592(4)−2.608(3) |
| mean | 2.601(4) | 2.594(7) | 2.599(5) |
| Re−S | 2.387(8)−2.418(8) | 2.368(15)−2.421(13) | 2.369(16)−2.432(14) |
| mean | 2.403(9) | 2.396(12) | 2.40(2) |
| Re−X | 2.448(10)−2.457(9) | 2.579(6)−2.606(6) | 2.781(5)−2.790(6) |
| mean | 2.451(4) | 2.595(10) | 2.786(3) |
| Re−Re−Re[d] | 59.8(1)−60.2(1) | 59.6(1)−60.4(1) | 59.8(1)−60.3(1) |
| mean | 60.0(1) | 60.0(2) | 60.0(1) |
| Re−Re−Re[e] | 89.9(1)−90.1(1) | 89.8(1)−90.2(1) | 89.9(1)−90.1(1) |
| mean | 90.0(1) | 90.0(1) | 90.0(1) |
| Re−Re−S | 56.9(2)−57.6(2) | 56.5(4)−58.1(3) | 56.4(4)−58.1(3) |
| mean | 57.2(2) | 57.2(4) | 57.3(4) |
| Re−Re−X | 132.8(2)−137.1(2) | 132.3(2)−137.6(2) | 133.0(1)−136.8(2) |
| mean | 135(1) | 135(1) | 135(1) |
| Re−S−Re | 65.2(2)−65.9(2) | 64.9(3)−66.1(4) | 64.7(4)−66.4(3) |
| mean | 65.5(2) | 65.5(3) | 65.5(4) |
| S−Re−S | 89.2(3)−90.2(3) | 88.8(5)−90.6(5) | 88.5(6)−90.9(5) |
| mean | 89.8(3) | 89.8(5) | 89.8(6) |
| S−Re−X | 91.7(3)−95.2(3) | 91.4(4)−95.5(3) | 91.2−95.2 |
| mean | 93(1) | 93(1) | 93(1) |

[a] From $(Bu_4N)_4[Re_6S_8Cl_6]$. [b] From $(Bu_4N)_4[Re_6S_8Br_6]\cdot H_2O$. [c] From $(Bu_4N)_4[Re_6S_8I_6]\cdot H_2O$. [d] Within triangular faces. [e] Within equatorial squares.

Interatomic distances and angles are summarized in Table 10; comparison with their solid-state precursors (Table 8) does not reveal any meaningful differences in cluster geometry. $Cs_4Re_6Se_8I_6$ dissolves in aqueous HI to yield a bright red solution. Basifying the solution with KOH results in a color change to yellow. Preliminary experimentation suggests that the change is due to a complete exchange of $OH^-$ for terminal $I^-$ ligands, to give the cluster $[Re_6Se_8(OH)_6]^{4-}$. Although the exchange curtails a direct preparation of $[Re_6Se_8I_6]^{4-}$, this species should be readily accessible by reaction of its protonated form ($[Re_6Se_7(SeH)I_6]^{3-}$, described below) with an appropriate sterically hindered base. No evidence of a similar ligand substitution was observed for the $[Re_6S_8X_6]^{4-}$ (X = Cl, Br) cluster analogues; however, such an exchange might partially account for the low yields attained in preparing $(Bu_4N)_4[Re_6S_8I_6]\cdot H_2O$.

Treatment of $[Re_6S_8X_6]^{4-}$ (X = Cl, Br, I) with acid in a nonaqueous solvent such as acetonitrile reversibly protonates the cluster cores in accordance with the following formal reaction.

$$[Re_6S_8X_6]^{4-} + H^+ \rightleftharpoons [Re_6S_7(SH)X_6]^{3-} \qquad (12)$$

The protonation, which may be accomplished using HX, as well as a variety of other anhydrous acids, induces an immediate color change to red (X = Cl, Br) or red-brown (X = I). The color change is never observed in aqueous solutions, implying

**Table 11.** Selected Interatomic Distances (Å) and Angles (deg) for $[Re_6S_7(SH)X_6]^{3-}$ (X = Cl, Br, I)

| | $[Re_6S_7(SH)Cl_6]^{3-}$ [a] | $[Re_6S_7(SH)Br_6]^{3-}$ [b] | $[Re_6S_7(SH)I_6]^{3-}$ [c] |
|---|---|---|---|
| Re−Re | 2.591(2)−2.608(2) | 2.593(2)−2.606(2) | 2.597(3)−2.612(3) |
| mean | 2.599(5) | 2.600(4) | 2.604(5) |
| Re−S | 2.377(7)−2.424(6) | 2.381(10)−2.248(9) | 2.378(13)−2.412(10) |
| mean | 2.407(11) | 2.403(10) | 2.398(9) |
| Re−X | 2.413(6)−2.429(8) | 2.554(4)−2.577(4) | 2.753(4)−2.763(3) |
| mean | 2.419(6) | 2.568(9) | 2.759(4) |
| Re−Re−Re[d] | 59.7(1)−60.3(1) | 59.8(1)−60.3(1) | 59.8(1)−60.3(1) |
| mean | 60.0(2) | 60.0(1) | 60.0(2) |
| Re−Re−Re[e] | 89.7(1)−90.3(1) | 89.6(1)−90.4(1) | 89.5(1)−90.5(1) |
| mean | 90.0(2) | 90.0(2) | 90.0(4) |
| Re−Re−S | 56.5(2)−57.9(1) | 56.7(2)−57.9(2) | 56.6(3)−57.7(3) |
| mean | 57.3(3) | 57.3(3) | 57.1(3) |
| Re−Re−X | 133.2(1)−136.8(2) | 132.6(1)−137.4(1) | 133.0(1)−136.8(1) |
| mean | 135(1) | 135(1) | 135(1) |
| Re−S−Re | 64.7(2)−66.0(2) | 64.9(2)−65.9(2) | 65.4(3)−66.1(3) |
| mean | 65.4(3) | 65.5(2) | 65.7(3) |
| S−Re−S | 89.1(2)−90.4(2) | 88.7(3)−90.5(3) | 89.1(4)−90.4(4) |
| mean | 89.8(4) | 89.8(4) | 89.8(4) |
| S−Re−X | 91.4(2)−95.4(2) | 90.9(3)−95.6(3) | 91.7−95.5 |
| mean | 93.3(9) | 93(1) | 94(1) |

[a] From $(Bu_4N)_3[Re_6S_7(SH)Cl_6]$. [b] From $(Bu_4N)_3[Re_6S_7(SH)Br_6]\cdot 2Me_2CO$. [c] From $(Bu_4N)_3[Re_6S_7(SH)I_6]\cdot 2Me_2CO$. [d] Within triangular faces. [e] Within equatorial squares.

that $[Re_6S_8X_6]^{4-}$ is a weaker base than $H_2O$. The reagents $SOX_2$ (X = Cl, Br) provide a useful means of generating HX while simultaneously removing any unwanted water. The presence of *three* $(Bu_4N)^+$ cations in the crystal structures of the protonated products $(Bu_4N)_3[Re_6S_7(SH)Cl_6]$, $(Bu_4N)_3[Re_6S_7(SH)Br_6]\cdot 2Me_2CO$, and $(Bu_4N)_3[Re_6S_7(SH)I_6]\cdot 2Me_2CO$ indicates that just one proton is associated with each cluster. The geometric details from these structures are reported in Table 11. Comparison with the unprotonated cluster (Table 10) exposes a slight shortening in the Re−X bond lengths—consistent with the increase in overall core charge—as the only noteworthy difference.[52] When precipitated with $(Bu_4N)I$ from an acidic aqueous solution of $Cs_4Re_6Se_8I_6$, the $[Re_6Se_8I_6]^{4-}$ cluster protonates under similar conditions, ultimately affording crystalline black $(Bu_4N)_4[Re_6Se_7(SeH)I_6]\cdot 2Me_2CO$. Interatomic distances and angles for the structure of the latter are included in Table 7.

In solution, electronic absorption spectra (Figure 10) provide a clear means of distinguishing the protonated and unprotonated cluster species. Note the correspondence between peaks in the spectra of the chloride- and bromide-ligated clusters: the positions of the latter are slightly red-shifted from those of the former. Although the peaks are not as well resolved, this trend in band shifts may be extrapolated to the iodide-ligated clusters (*e.g.*, $\lambda_{max}$ = 434, 443, and 507 nm for $[Re_6S_8X_6]^{4-}$ with X = Cl, Br, and I, respectively), indicating that the bands are likely due to halide ligand-to-metal charge transfer. A spectrophotometric titration of $[Re_6S_8Br_6]^{4-}$ with anhydrous perchloric acid in acetonitrile confirmed the uptake of no more than one proton per cluster. Further, titration of $[Re_6S_7(SH)Br_6]^{3-}$ with triethylamine in acetonitrile allowed its p$K_a$ to be estimated at 20 (the p$K_a$ of $Et_3NH^+$ in acetonitrile is 18.5).[53] Thus, consistent with their high negative charge, these clusters exhibit considerable basicity in aprotic solvents such as acetonitrile. Indeed, yellow acetonitrile or dichloromethane solutions of $[Re_6S_8X_6]^{4-}$ (X = Cl, Br) gradually turn red over the course of 1 or 2 days when exposed to air ($H_2O$ and $CO_2$). In water, on the other hand, the clusters are not demonstrably basic (presumably due to the inability of a protonated cluster to act as a hydrogen-bond donor), and their solutions remain yellow in air for periods of >3 months. The cyclic voltammetry of the $[Re_6S_8X_6]^{4-}$ (X = Cl, Br) clusters in acetonitrile reveals a reversible one-electron oxidation wave at $E_{1/2}$ = +0.27 and +0.31 V, respectively, and remarkably similar voltammograms are observed for solutions of their protonated analogues. Direct characterization of the SH moiety in $(Bu_4N)_3[Re_6S_7(SH)Br_6]\cdot 2Me_2CO$ could not be elicited from either its $^1H$ NMR ($CD_3CN$; no evidence for paramagnetism) or infrared (KBr) spectra.

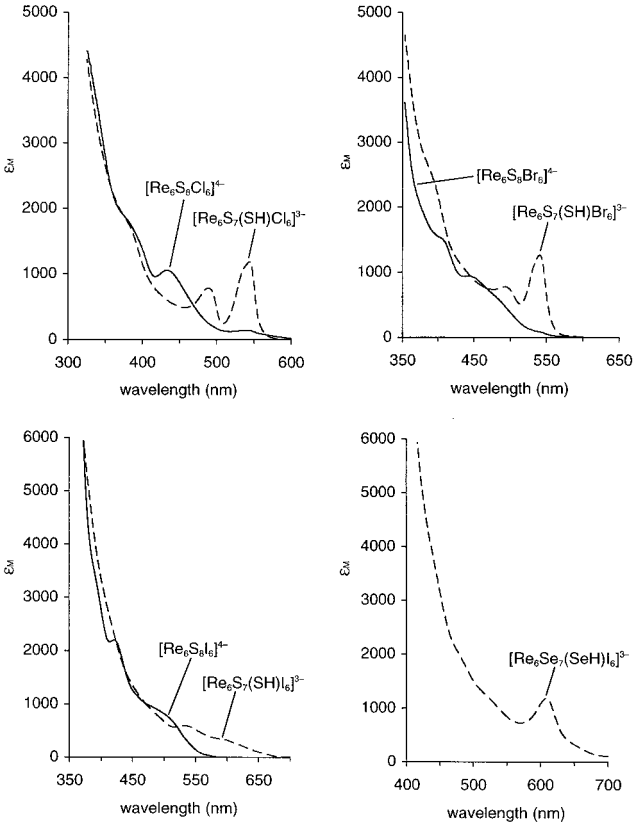


**Figure 10.** Absorption spectra for acetonitrile solutions of $[Re_6S_8X_6]^{4-}$ (solid line) compared with $[Re_6S_7(SH)X_6]^{3-}$ (dashed line) and $[Re_6Se_7(SeH)I_6]^{3-}$.

There exists scant precedent in metal−chalcogenide cluster chemistry for core protonation reactions of the type established

(52) The absence of any metric differences in S atom coordination is not surprising, since the core proton could not be located in any of these structures and is almost certainly disordered over all eight possible sites.

(53) Coetzee, J. F.; Padmanabhan, G. R. *J. Am. Chem. Soc.* **1965**, *87*, 5005.

here. The most closely related examples involve the reversible uptake of a single proton by the cubane clusters $[Fe_4Q_4(Q'R)_4]^{2-}$ (Q, Q′ = S, Se) in aqueous solution.[54] Fully protonated cubanes $[M_4(SH)_4(CO)_{12}]$ (M = Mn, Re) have also been reported, but were not demonstrated to undergo deprotonation.[55] Otherwise, there are only a few dinuclear examples of relevance, and in these cases, protonation is generally accompanied by some rather severe structural changes.[56] Given the current level of reliance upon single-crystal X-ray diffraction techniques for characterizing new cluster compounds, it seems probable that there are other examples in which the protonation of a highly-charged anionic metal−chalcogenide cluster may have gone undetected. For instance, in light of the above results (as well as the synthetic procedures and means of characterization employed), it appears plausible that the ruby red cluster previously identified as $[Re_6S_6Cl_8]^{2-}$ [8a] might actually correspond to $[Re_6S_6(SH)Cl_7]^{2-}$ formed by protonation of $[Re_6S_7Cl_7]^{3-}$ in acetonitrile upon exposure to air.

## Summary

Many transition metal clusters have been exclusively attained in solid phases as integral components of extended covalent frameworks that are not amenable to breakup by means of conventional cluster excision techniques. Dimensional reduction, a general approach for deconstructing extended solid frameworks, is described in detail, and its effectiveness in liberating clusters from such environs is demonstrated by application to a number of intractable $[Re_6Q_8]^{2+}$ (Q = S, Se) core-containing phases. The following are the principal results and conclusions from this endeavor.

(1) The concept of dimensional reduction is exemplified in Figure 3 with the stepwise dismantling of a simple three-dimensional framework, $MX_3$. Each additional equivalent of X incorporated in the structure serves to terminate the bridges in one dimension, resulting in two-dimensional sheets, one-dimensional chains, and ultimately, discrete molecules. The charge built up in this process is compensated by the simultaneous incorporation of cations, A, residing external to the anionic framework. Thus, the connectedness (and, less rigorously, the dimensionality) of a solid framework can be predictably reduced with the controlled insertion of AX. This formalistic approach may be used for targeting solid-state reaction products featuring lower-dimensional, less tightly-bound frameworks. Further, by replacing metal centers M with multinuclear cluster cores $[M_mQ_q]$, it is readily extended to include cluster-containing frameworks.

(2) Equation 6 summarizes the dimensional reduction of $Re_6Se_8Cl_2$ (Figure 2; this two-dimensional structure features rhombic $Re_2Se_2$ linkages of the type common to many intractable cluster phases) via incorporation of TlCl. As expected, the new phases encountered exhibit cluster frameworks of reduced connectedness and dimensionality: two-dimensional $[Re_6Se_8Cl_3]^{1-}$ sheets, one-dimensional $[Re_6Se_8Cl_4]^{2-}$ chains, and discrete $[Re_6Se_8Cl_6]^{4-}$ clusters. Frameworks of the latter two types are also observed in the dimensional reduction of three-dimensional $Re_6S_8Cl_2$ (Figure 4) with TlCl.

(3) In pursuit of a directly soluble form of the $[Re_6Se_8]^{2+}$ cluster core, cesium halides were employed as dimensional reduction agents (eqs 7 and 8). The insoluble one-dimensional chain phases $Cs_2Re_6Se_8X_4$ (X = Cl, Br; Figure 6) are the sole cluster products with use of CsCl and CsBr. However, reactions with CsI enable isolation of two-dimensional $CsRe_6Se_8I_3$ (Figure 7) and, finally, the soluble molecular phase $Cs_4Re_6Se_8I_6$ (Figure 8). A similar strategy permits synthesis of soluble phases containing the $[Re_6S_8]^{2+}$ core: $Cs_5Re_6S_8X_7$ (X = Cl, Br; Figure 9) and $Cs_6Re_6S_8I_8$.

(4) The possible connectivities for frameworks featuring $[M_6Q_8]$ clusters are enumerated in Table 9. Of the 28 possibilities, 10 have been observed, and three are unique to novel $[Re_6Q_8]^{2+}$ (Q = S, Se) core-containing phases described herein.

(5) The compounds $Cs_5Re_6S_8X_7$ (X = Cl, Br) and $Cs_6Re_6S_8I_8$ dissolve in aqueous base to afford yellow solutions of their respective $[Re_6S_8X_6]^{4-}$ clusters. Addition of $(Bu_4N)X$ yields the $(Bu_4N)^+$ salts of these molecular clusters in solid forms conveniently soluble in polar organic solvents; selected cluster interatomic distances and angles resulting from the single-crystal X-ray analysis of each salt are set out in Table 10 for comparison. Rapid substitution of hydroxide for the terminal iodide ligands on the cluster prevents isolation of an analogous species from basic solutions of $Cs_4Re_6Se_8I_6$.

(6) Yellow acetonitrile solutions of $[Re_6S_8X_6]^{4-}$ (X = Cl, Br, I) react with anhydrous HX to give red solutions of the singly protonated clusters $[Re_6S_7(SH)X_6]^{3-}$, as evidenced by spectrophotometric titrations, single-crystal X-ray structure determinations, and elemental analyses. The red-brown species $[Re_6S_7(SeH)I_6]^{3-}$ is also obtained with an analogous workup of red, *acidic* aqueous solutions of $Cs_4Re_6Se_8I_6$.

Results (2), (3), and (5) above clearly demonstrate the utility of the dimensional reduction approach (1) in deconstructing tightly-bound cluster frameworks and accessing their core components in soluble molecular form. With entry to $[Re_6Q_8]^{2+}$ core-containing clusters, their molecular chemistry can now be disclosed. Studies directed toward this end are in progress.

**Acknowledgment.** This work was funded by the National Science Foundation (Grants CHE 92-0387 and 94-3830). We thank the Office of Naval Research for supporting J.R.L. (predoctoral fellowship, 1991−94), Andrew S. Williamson and Craig C. McLauchlan for experimental assistance, and David Lange and Bernie Souza for technical assistance.

**Supporting Information Available:** X-ray structural information for the compounds in Tables 3−5, including tables of crystal and intensity collection data, positional and thermal parameters, and interatomic distances and angles (101 pages). Ordering information is given on any current masthead page.

JA960216U

(54) (a) Bruice, T. C.; Maskiewicz, R.; Job, R. *Proc. Nat. Acad. Sci. U.S.A.* **1975**, *72*, 231. (b) Nakamoto, M.; Tanaka, K.; Tanaka, T. *Bull. Chem. Soc. Jpn.* **1988**, *61*, 4099.

(55) Küllmer, V.; Vahrenkamp, H. *Chem. Ber.* **1976**, *109*, 1560.

(56) Kramarz, K. W.; Norton, J. R. *Prog. Inorg. Chem.* **1994**, *42*, 1 and references therein.